UTILIZATION OF LOW ALTITUDE REMOTE SENSING TECHNIQUES FOR CORAL BLEACHING ASSESSMENTS

A THESIS SUBMITTED TO THE GRADUATE DIVISION OF THE UNIVERSITY OF HAWAI‘I AT MĀNOA IN PARTIAL FULFILMENT OF THE REQUIREMENTS FOR THE DEGREE OF

MASTER OF SCIENCE

IN

BIOLOGY (MARINE SCIENCE)

DECEMBER 2016

By

Joshua Levy

Thesis Committee:

Cynthia Hunter, Chairperson

Eric Hochberg

Robert Bidigare

Keywords: *coral reef, remote sensing, coral bleaching, unmanned aerial systems*

ACKNOWLEDGEMENTS

I thank Dr. Erik Franklin for the use of his image processing and spatial analysis resources. Thanks to Dr. Oscar Sosa for his skills and resources that allowed for efficient phosphate analysis. Raphael Ritson-Williams was vital for the collection and processing of environmental stressor data. Thanks to Dr. Trent Lucaczyk for helping edit the technical sUAS information. Thanks to Ted Ralston for helping us navigate the various FAA regulations. A special thanks to all of the field assistants who aided with aircraft retrieval and GCP collections during the reef surveys.

ABSTRACT

The utilization of small-unmanned aerial systems (sUAS) as a cheap, effective complement to other assessment tools is imminent in the field of coral reef ecology. Here, we describe the current status of sUAS in the field of coastal monitoring, and introduce the utilization of low-altitude sUAS assessments for coral reef research using proof-of-concept results and completed work describing the distribution of coral bleaching across several patch reefs in Kāneʻohe Bay, Hawaii. Overlapping sub-centimeter reef imagery collected during the 2015 coral bleaching event was used to construct complete high-resolution reef images of four Kāneʻohe Bay patch reefs located in "long residence time" and "short residence time" flow regimes. The spatial distributions of bleached and paled corals were assessed in relation to coastal stressors (sedimentation rates, salinity and phosphate concentrations). Results support the notion that phosphate, an important inorganic nutrient, differed significantly between "closer to shore" and "further from shore" reefs instead of between previously determined flow regimes. Mean phosphate concentrations and salinities were both significantly correlated to unhealthy (bleached or paled) coral cover. When assessing the environmental conditions in close temporal proximity to image collection, only salinity had a strong negative correlation with the cover of unhealthy coral. Paled, bleached, and healthy coral on all four reefs were significantly clumped spatially, although bleached corals had the largest mean distances between affected colonies. This project provides valuable insight into the relationships between Kāneʻohe Bay patch reefs and coastal stressors at previously unexplored spatial scales, and demonstrates the effective use of sUAS surveys in the field of coral reef science.

TABLE OF CONTENTS

ACKNOWLEDGEMENTS i

ABSTRACT ii

LIST OF TABLES v

CHAPTER I 1

Introduction 1

UAS 5

Choosing Survey Techniques 9

Sensor Specifications 10

Flight Planners 10

Field Operations 11

Post-Processing 12

Geo-referencing 12

Ground-Truthing 13

Results 13

Applications 14

Limitations 15

FAA Regulations 17

Conclusion 19

CHAPTER II 21

Introduction 21

Coral Bleaching 22

Study Site 22

2015 Bleaching event 23

Coral Bleaching Survey Techniques 28

Methods 30

Pre-flight procedure 30

Flight Operations 31

Environmental Parameters 32

Analysis 33

Image processing 33

Ground Truthing 33

Image Classification 33

Spatial and Statistical Analysis 34

Results 35

Between-Reef Environmental Variability 35

Within-Reef Variability 36

Coral Health 36

Time Lags 36

Spatial Statistics 36

Discussion 37

Coastal Stressors 37

Survey Methodology Comparison 38

Coral Health Response to Coastal Stressors 39

Spatial Analysis 40

General Conclusions 41

Limitations 42

Conclusion **45**
TABLES **47**
FIGURES **52**
LITERATURE CITED **67**

LIST OF TABLES

Table 2.1. Patch reef area and coral cover. Excerpt from Nielson et al [23]. 47
Table 2.2. Coral health categorized into percent healthy, unhealthy, and total coral cover by reef.....48
Table 2.3. Z-scores and search thresholds of Moran's I spatial autocorrelation test.....49
Table 2.4. Mean patch ENN values by reef and coral health. Standout values are bolded. 50
Table 2.5. Patch reef coral cover comparing *in situ* and sUAS survey techniques. *In situ* data was collected by DAR from February-April, 2014 [23]. sUAS data was collected from August-October 2015. Amount overestimated by *in situ* analysis is underlined. 51

LIST OF FIGURES

Figure 1.1. UAS survey of Kaneohe Bay Patch Reef 44 at 20m altitude on 1/20/2015. Total reef area 47,000 m^2. a) 35 m^2 subset demonstrating colony-level resolution. b) Satellite imagery of same reef area. 52
Figure 2.1. Kāneʻohe Bay satellite imagery with an overlay of associated flow regime areas as described by Lowe et al. 2009. The four patch reefs targeted in this study are highlighted. 53
Figure 2.2. Ground-truth verification of aerial imagery. a) Aerial image of healthy coral and non-coral substrate inside the 1m^2 quadrat at 20m altitude. b) Cropped aerial image to isolate the quadrat. c. *In situ* imagery of the quadrat. Note the insufficient image coverage of the *in situ* quadrat due to shallow reef depth. 54
Figure 2.3. Example of rubble/non-coral substrate. a) 1m^2 *in situ* quadrat. b) 1m^2 crop of aerial imagery 55
Figure 2.4. Comparison of aerial and *in situ* imagery to verify substrate class. a) Aerial image taken from 20m altitude of healthy coral (top right) and dead coral/non-coral substrate (center). b) *In situ* imagery of the healthy coral and dead coral/non-coral substrate across the transect line. 56
Figure 2.5. Coastal stressor values between patch reefs. a) Salinity, b) Sedimentation rate, c) Phosphate. 57
Figure 2.6. Within–reef coastal stressor values. a) Local variation in sedimentation rates by reef ($p = 0.0128$). b) Local variation in sedimentation rates by block ($p = 0.8674$). 58
Figure 2.7. Beta model assessing Healthy and Unhealthy coral by the standard deviation of: a, d) Salinity, b, e) Sedimentation Rate, and c, f) Phosphate respectively. 59
Figure 2.8. Beta model assessing Healthy and Unhealthy coral by mean: a, d) Salinity, b, e) Sedimentation rate, and c, f) Phosphate concentration respectively. 60
Figure 2.9. Beta model assessing Unhealthy coral at the last time point before reef imagery was collected: a) Salinity, b) Sedimentation rate, c) Phosphate concentration. 61
Figure 2.10. Assessing variance of Euclidean Neareast Neighbor values by health type and reef. 62
Figure 2.11. Spatial analysis workflow for Reef 20. Pixel size: 0.009x0.009 m. a) Reef mosaic with inset. b) Orthomosaic classified into three coral health states and non-coral substrate. c) Heat map of paled colony clusters with environmental sample station locations. d) Heat map of bleached colony clusters with water sample locations 63
Figure 2.12. Spatial analysis workflow for Reef 25. Pixel size: 0.033x0.033 m. a) Reef mosaic with inset. b) Orthomosaic classified into two coral health states, sand, and non-coral substrate. c) Heat map of bleached colony clusters with environmental sample station locations. 64
Figure 2.13. Spatial analysis workflow for Reef 42. Pixel size : 0.021x0.021 m. a) Reef mosaic with inset. b) Orthomosaic classified into three coral health states

and non-coral substrate. c) Heat map of paled colony clusters with environmental sample station locations. d) Heat map of bleached colony clusters with water sample locations. Water sample station C was located beyond extent of reef imagery. 65

Figure 2.14. Spatial analysis workflow for Reef 44. Pixel size: 0.007x0.007 m. a) Reef mosaic with inset. b) Orthomosaic classified into three coral health states and non-coral substrate. c) Heat map of paled colony clusters with environmental sample station locations. d) Heat map of bleached colony clusters with water sample locations. Water sample station C was located beyond the areas of reef imagery. 66

LIST OF ABBREVIATIONS

UAS- Unmanned aerial systems

sUAS- Small unmanned aerial systems

SfM- Structure from motion

PDO- Pacific decadal oscillation

GCP- Ground control points

GPS- Global positioning system

ENVI- Environment for Visualizing Images

ENN- Euclidean nearest neighbor

RGB- Red, green, blue

MCBH- Marine Corps Base Hawaii

AGL - At ground level

RPC - Remote pilot certificate

NAS- National Air Space

CHAPTER I

Unmanned Aerial Systems for Coral Reef Science: An Introduction and Case Study
(Submitted to the Journal of Coastal Research)

Introduction

Jacques Cousteau envisioned that technology such as satellites, aircraft, instrumented buoys, and other manned or unmanned devices might someday replace the inefficient and expensive method of gathering ocean data via ships. While many oceanographic projects have already adopted the use of such technologies to provide more accurate, comprehensive data about the world's oceans, we are only just beginning to explore the applications of new technologies for biological marine sciences. Coral reefs are biodiversity hotspots that are vital to the function of global economic and biologic processes. Due to the inherent heterogeneity, size, and, in some cases, remoteness of coral reefs, it is difficult to routinely monitor their dynamics at functionally important spatial scales. We argue that small-unmanned aerial vehicles (sUAS) are efficient, cost-effective tools for monitoring fine-scale reef dynamics over a wide range of spatial (cm-km) and temporal scales (hourly-annually).

Coral reefs provide a variety of ecosystem functions ranging from essential fish habitats to natural breakwaters that are vital to the sustainability of countless coastal communities throughout the tropics. From an economic perspective, reefs, which sustain these ecosystem services and thriving tourism industries, have an estimated global value of $29.8 billion per year[1]. Coastal and global stressors have an additive, negative impact on coral health[2]. Global stressors such as elevated temperatures and ocean acidification, and coastal stressors such as runoff, pollution, tourism overuse, and unsustainable fishing

reduce coral reef resilience, promote algal overgrowth and increase coral mortality[3–7]. As we continue to populate coastlines and change the global climate at a rapid rate, corals may not be able to adapt[8]. In order to help mitigate the steadily declining trend in global coral health, it is imperative that we collect information at biologically relevant spatial scales to monitor reef health and understand how global and local stressors impact reef dynamics. This information will help create and/or amend management strategies that will more effectively protect these fragile yet vital marine ecosystems from further degradation.

Information can be collected on various spatial scales to answer questions that range from coral reproductive physiology to regional reef resilience mapping[9–11]. For management applications, it is important to understand how a stressor can impact a reef at various spatial scales. Although observing single polyp or colony responses to such stressors is useful to understanding physiological processes, these do not provide a comprehensive view of the organism's functioning within its ecosystem. Therefore, it is important to assess the health of that single polyp or coral colony within the reef or ecosystem context.

The way we collect reef information depends on the spatial scale in question. The two general ways we collect reef information are via *in situ* or remote sensing techniques. After reviewing nine methods used for *in situ* surveys, Jokiel et al. (2005) identified underwater photo transects as the most efficient method at collecting high-resolution reef information at local scales[12]. Jokiel et al. (2005) also brought attention to the importance of power analysis and large sample sizes for methodologies used in monitoring or assessment projects[12]. Ideally, an optimal method would document higher species counts,

moderate area coverage, and low variance to increase the survey accuracy[12]. To further this point, reef community structure is extremely heterogeneous over scales of centimeters to hundreds of meters[13]. Therefore, conducting an *in situ* assessment over a fraction of one reef will not necessarily be an accurate representation of the reef as a whole. Additionally, some reefs are situated where remoteness, weather conditions, or reef topography prohibit the safe, routine collection of *in situ* reef information. Over the past two decades, the development of remote sensing techniques has allowed marine scientists to efficiently collect large-scale reef information in such environments[14].

Direct remote sensing is defined as the ability to detect individual organisms, species, assemblages, or ecological communities from satellites or airplanes[15]. This technique has been applied to coastal marine assessments for sea level rise, baseline/routine monitoring, and environmental sensitivity mapping of sea grasses, mangroves, algae, aquaculture, and coral reefs[16]. It is important for remote sensing systems to spatially and spectrally resolve functional reef bottom-types such as sand, coral, sea grasses, algae, and rubble[17]. Current methods use spectral classifications to quantitatively discriminate between substrates via the distinct spectral signature characteristics of each substrate type[15,18,19] .

Spectral classification is the process of categorizing image pixels into classes, or into a fractional representation of the relative contributions from different spectral endmembers[20]. Imaging with multi-spectral or hyper-spectral sensors is capable of simultaneously collecting information on tens or hundreds of separate bands of light over a large range of wavelengths to collect information on water properties, bathymetry and benthic composition[18,21,22]. This technology is especially important in reef environments,

as it allows for differentiation between very small changes in spectral reflectance, and can therefore tease apart subjects that have similar spectral properties. For instance, collecting narrow-band (20 nm), multispectral imagery between 480 and 540 nm can be used to distinguish between functionally distinct corals and algae that are visually indiscernible in RGB remote sensing data[20]. When used *in situ*, spectral sensors can give reef scientists the ability to assess coral pigment levels and symbiont densities[19,24]. However, the coarse resolution of these sensors on airborne and satellite remote sensing platforms, and the poor spatial resolution inherent with multispectral sensors in comparison to RGB sensors, do not allow for the fine-scale spatial discrimination between reef components that is required for some coral reef applications[20,25].

Remote sensing surveys have contributed enormously to the characterization of coral reefs by providing previously unattainable large-scale reef information[26]. However, there are temporal, spatial, and monetary limitations that are particularly apparent when trying to answer certain biological questions. Costs of obtaining multiple sets of imagery, the temporal gap between satellite passes for repeat surveys, radiometric corrections necessary to standardize image color and brightness, and the inability to resolve to some biologically relevant spatial scales inhibit the use of remote sensing techniques to answer questions that require colony-level resolution over large areas [16,26].

Considering that *in situ* and remote sensing techniques are collecting reef information at the two edges of the spatial spectrum, another methodology must be utilized to collect intermediate-scale reef information. In order to obtain high resolution, large-scale reef information, RGB imagery or spectral information must be collected at lower altitudes.

Unmanned aerial platforms were first used to map reef environments in 1978 with the use of helium balloons, and later with kites in 1982[27,28]. Both of these methods utilized tethered aerial platforms equipped with a camera and trigger mechanism to obtain consecutive, overlapping low altitude aerial images of reef areas at an altitude of 40-50 m[27,28]. Although these techniques were advanced for their time, the amount of area mapped was limited to the length of the tether and mobility of the kite operator to cover as much ground as possible. Current unmanned aerial platforms are self-powered, untethered systems that allow for more freedom in low altitude aerial mapping efforts.

UAS

Unmanned aerial systems, UAS, or drones, offer a viable alternative to traditional platforms for acquiring high-resolution remote-sensing data at lower cost, increased operational flexibility, and greater versatility. The recent surge in commercial production of small UAS's (sUAS) has increased the accessibility of these platforms to various hobbyist, commercial, and research applications. sUAS are defined as fixed wing or multi-rotor aircraft that weigh less than 25 kg and are flown without a pilot in the cockpit[29,30].

The quad-copter is a popular, stable, multi-rotor design that uses two sets of identical fixed-pitch propellers for lift and propulsion. Control of vehicle motion is achieved by altering the rotation rate of the rotor discs, and an electronic control system and sensor arrays stabilize the aircraft. The four-rotor design allows quad-copters to be relatively simple in design yet highly maneuverable and reliable. Compared to a traditional helicopter, the lack of mechanical linkages otherwise needed to vary the pitch angle of the rotor blade simplifies the design and maintenance of the vehicle; the use of smaller and lighter propellers improves the safety of the vehicle[23]. The need for aircraft

with greater maneuverability and hovering ability due to limited launch and landing space during field operations has led to a rise in quad-copter use in environmental monitoring and mapping[30]. Quad-copters have a major advantage over fixed-wing aircraft because they can hover, fly at slow speeds, and change altitude with no horizontal motion[30]. This allows for the collection of very low altitude imagery with minimal forward motion distortion and easily enables mapping at consistent spatial resolutions. However, due to aerodynamic limitations, quad-copter and other multi-rotor designs have shorter flight capabilities than fixed-wing aircraft.

Fixed wing sUAS refer to vehicles configured similar to a passenger airplane. Typically they are composed of a fuselage, a main wing and a thrusting propeller. Many configurations of fixed wings exist. One popular configuration is the "flying wing," composed of one large wing blended with a fuselage in the middle that holds electronics and sensors. Another popular design is the "conventional" configuration, which in addition to a main wing and fuselage uses an "empennage," or tail to control the pitch and yaw rotations. In the context of mapping, a primary strength of the fixed wing UAS is its endurance. Typically a sUAS fixed wing aircraft can fly between 45 minutes and 120 minutes. This is a critical feature needed for mapping large areas such as coral reefs.

A main challenge for the deployment of fixed wing UAS is the operational complexity associated with launching and landing. Launching a small fixed wing craft is generally simple, and can be accomplished by throwing it like a paper airplane. Larger fixed wings need either a runway, or more commonly a catapult. Landing fixed wings regardless of size is generally the most difficult part of the mission and requires the most expertise. In order to safely land, many considerations are made for approaching a

landing site. First, the distance needed to descend and align the aircraft with a landing zone can be quite long, affecting the flight path and the pilot's focus for several minutes before the actual landing occurs. Second, the effect of environmental factors like wind adds complexity by requiring a pilot to choose an approach heading into the wind, or landing with a side-slip. Third, to account for all the variables involved, a long area of (dry) land is needed to receive the vehicle during touch-down. Compared to a multi-rotor craft, the complexity of this operation is many times greater and is typically the major barrier to entry for a new operation. This would explain why fixed wing deployments are still rare in ocean research applications.

sUAS are easily transportable aerial platforms that can carry lightweight sensors (~3 kg) and fly at low altitudes with a high degree of control under autonomous flight. sUAS guided by autonomous flight systems have the capacity to fly "low and slow" to obtain clear, hyperspatial (<10 cm pixel size) imagery of targeted areas with minimal atmospheric noise[29,31]. Improvements in the design of flight control systems have transformed sUAS platforms into research-grade tools capable of acquiring high-quality images of geophysical/biological dynamics[30].

Much like the use of airborne sensors in the early 2000s, the scientific community is starting to understand the potential for UAS-mounted sensors for assessing tropical environmental resources. sUAS platforms were first used by wildlife biologists for monitoring and inventorying wildlife in areas inaccessible by foot[32]. Because revisit times are determined by the operator as opposed to fixed satellite revisit times, geologists utilized sUAS to conduct fine-scale temporal assessments to detect landslides, map fault zones, and volcanic activity[32,31]. The lower costs, human risks, ecological footprint,

radiometric corrections, and improved spatial resolution compared to traditional remote sensing techniques have led to the use of sUAS in several fields of coastal marine ecology including wildlife surveys, wetland assessments, coastal erosion assessments, and coral reef surveys[30,33–36].

Most of the examples above use sUAS to fly high altitude (100-300 m), high speed operations to collect information about large areas. At this height, depending on the sensor and lens used, image resolution obtained is 3-10 cm. Although this is considered high resolution for aerial imagery, the spatial resolution required depends on the study subject and biological question at hand, and therefore varies by project. Coral reef surveys that require species-specific information about coral and algal benthic components should resolve down to the coral colony scale. Coral colony size can vary significantly between species and between individuals of the same species, so it is important to collect imagery at the finest resolution possible in order to identify as many individual coral colonies or algal patches as possible. At lower altitudes, flights become less efficient, as the area photographed decreases, and the sensor must travel at slower speeds to collect non-blurry images. Additionally, at very low altitudes (~10-12 m) propeller turbulence can impact the water state and produce distortion artifacts. Our trial and error has determined that for low-end multi-rotor sUAS such as the DJI Phantom series, a "happy medium" altitude of 15-20 m provides 0.8-1 cm spatial resolutions using a 94° field-of-view RGB sensor. While this altitude provides adequate spatial resolution to easily collect colony-level information with the DJI Phantom series, minimum altitudes for acquiring such spatial resolution vary by platform size, and sensor type, quality, and zoom.

There is huge potential to utilize this platform for shallow-water benthic ecological surveys. Below is the workflow we utilized to produce a geo-referenced, sub-centimeter orthomosaic of a 50,000m^2 reef area with sUAS.

When planning a UAS reef survey, it is important to be knowledgeable of UAS capabilities, sensor options, flight planning software, and analysis tools that are available to answer your question. To illustrate this process, we will use the reef survey mentioned above as an example. While some of the methods below apply broadly to mapping efforts terrestrial or marine, which have been used in work such as Hodgson 2016, it is important to distill and describe a comprehensive workflow example, as it has not yet been accomplished in the peer-reviewed literature[37].

Choosing Survey Techniques

A survey was conducted to determine the population size and spatial distribution of the two dominant coral species, *Porites compressa* and *Montipora capitata*, on several patch reefs throughout Kaneohe Bay, Hawaii. Patch reefs in Kaneohe Bay range from 1000 m^2 to 50,000 m^2, with reef flats less than 2 m below sea level, and are located between 300 m and 3000 m from the nearest shore[38]. While some of these intermediate to small reefs could, and have, been surveyed manually using boat-launched snorkel methods, it is physically, monetarily and temporally exhaustive to conduct a spatially comprehensive survey of these reefs using such techniques. Additionally, snorkel surveys do not necessarily facilitate the actual mapping of all colony locations on each reef, as data are often not collected continuously, but rather at categorical intervals determined by the specific survey protocol[39]. A continuous mapping effort requires an aerial platform that is capable of launching from a small vessel, has a long battery life, and can carry a gimbaled, small, lightweight RGB sensor that faces at-nadir. While there are currently

many commercially-available multi-rotor sUAS, many are not optimized for field mapping efforts and are either too big to land on a small vessel, utilize non-gimbaled cameras that do not face at-nadir, or have flight times of less than 20 minutes. The DJI Phantom 3 Professional was employed for this project as it fits most of the criteria mentioned above.

Sensor Specifications

While some multi-rotor sUAS now come equipped with a built-in, gimbaled RGB sensor, others require the purchase of a separate camera and gimbal assemblage. Ideal cameras will have high megapixel sensors and wide-angled lenses to have the ability to capture maximum detail with maximum area coverage. However, post-processing steps to generate orthomosaics are computer intensive, so larger images files require longer processing times with limited resolution benefits. Generally, 12 megapixel cameras provide enough resolution while not being too computing intensive. It is also advised to avoid wide-angled lenses or cameras that have significant internal geometric errors such as fish-eye distortion. Although these distortions can be corrected using various software options, image accuracy is still compromised in comparison to "flat" lenses.

Flight Planners

There are several flight planning systems available that enable pre-programming of waypoints for automated flights. These systems allow for the precise control of location, speed, direction, and height of the platform during the flight in order to obtain the necessary resolution imagery of the area of interest. Flight planners such as eMotion, Mission Planner, DatuFly, and Drone Deploy vary in compatibility and ease-of-use, but all use similar interfaces to create flight plans on user-friendly satellite map layers, and all allow the operator to monitor flight paths in real time on laptops, smartphones, or

tablets. Some flight planning applications have the ability to upload flight plans to cloud servers, which makes it possible to create flight plans on one device and execute the flight on a different, field-optimized device.

Field Operations

Flight operations vary depending on reef proximity to land. If possible, it is always desired to launch and land the aircraft from shore. However, if the targeted reef is out of range of the remote control, or if reducing transit flight time can dramatically increase survey flight time, then launching from a boat is desirable. Boat operations require an open area either on the bow or stern, where the aircraft can launch and land either from the deck or by hand, if necessary. If compass calibrations are necessary, they should be performed before leaving shore, as metal on the boat can interfere with the compass. Internet connection is required to run the pre-planned flight plan unless it has been saved on a smartphone or tablet.

The aircraft is launched in autopilot mode using the flight planning application. Although not always required, it is beneficial to have a spotter maintain visual contact with the aircraft during the mission while the pilot monitors flight status on the device. Lost-connection protocol varies by flight planner but usually results in the aircraft continuing its programmed flight, as the waypoint data is loaded into the aircraft prior to takeoff. Although most modern sUAS will automatically set the “home location” as the launch coordinates, landing using the home coordinates is ill-advised on a floating vessel, as vessel location is constantly changing. Rather, taking manual control to land the aircraft on a flat surface or by hand is recommended.

Post-Processing

Depending on the flight planner, camera settings are either automated and controlled by the flight planning software or manually controlled by the pilot. When collecting still imagery, it is important to set the camera to a high frame rate capture in order to collect as much overlap across the y- axis between images as possible. If collecting video, it is important to utilize at least 1080p in order to maintain sufficient image quality. Still images can be batch edited to standardize image color and brightness to eliminate streaking or color inconsistencies. Video can be broken down into discrete single images and edited as above using image-processing software such as Adobe Photoshop and Lightroom. Software such as Agisoft Photoscan, which has been used successfully in terrestrial aerial mapping and *in situ* coral reef mapping, uses structure from motion (SfM) algorithms to estimate camera location at the point of each image's collection, then combines adjacent images within a scene to create orthomosaic models of a complete scene[40–42]. SfM techniques require ~60% overlap between images in both the x and y axes in order to produce accurate, undistorted orthomosaics[42].

Geo-referencing

In order to obtain accurate spatial and geographic information from the orthomosaics, it is necessary to geo-reference the composite image to a map coordinate system. Newer sUAS may have integrated sensors that embed geographic information into each image file, which yields a relatively straightforward georeferencing process for the orthomosaic. However, the GPS information collected by the UAS may not be as precise as desired. Therefore, it is always beneficial to manually geo-reference the mosaic using ground control points (GCPs) and GIS software such as ArcMap. Terrestrial georeferencing techniques use GCPs in addition to base stations, which collect GPS

coordinates of one location over an extended period of time to obtain a precise (5-10mm) GPS location[43]. While utilizing a similar system would decrease spatial error while georeferencing, it may not be feasible to deploy such equipment on remote reef areas. Temporary ground control points can be used to collect GPS coordinates across the reef. The GCPs must be visible in the mosaic to be effective in the georeferencing process. If it is necessary to compare sUAS imagery to common satellite products or to other sUAS imagery, it may be beneficial to geo-reference the aerial imagery visually by visually matching reef mosaics with satellite imagery.

Ground-Truthing

It is important to verify the accuracy of the aerial product via *in situ* ground-truthing. It is possible to conduct rapid *in situ* ground-truth assessments of small reef areas via video or photo imagery collected along a transect line. The transect line must be identifiable in the aerial imagery as a physical structure (transect tape or rope) or a series of GPS locations in order to obtain an absolute comparison of images of the same reef area collected via aerial and *in situ* methods. Another, more rapid alternative is to deploy several 1 m × 1 m quadrats onto the reef prior to the UAS flight, then collect *in situ* imagery of each quadrat post-flight. This allows for a side-by-side comparison of the aerial and *in situ* imagery.

Results

Using this workflow, we were able to collect colony-level reef imagery of a 50,000 m^2 reef within 30 minutes, and create a geo-referenced orthomosaic with sub-centimeter resolution (Figure 1.1).

Applications

Reef information collected using sUAS can be used to assess various metrics that are used as proxies to determine reef health, such as assessing changes in benthic community structure, size structure, and spatial range over time[8,17,44]. Additionally, UAS reef surveys can provide a large, and sometimes complete portion of a sample population, and thus describe spatial patterns that go undetected when using *in situ* surveys[31]. Such spatial patterns include species distributions, disease coverage, and bare substrate availability. This information provides a better understanding of reef dynamics and can help efficiently locate suitable substrate for coral restoration efforts. sUAS are an ideal tool for management organizations that are in need of cheap, accurate and unbiased tools to efficiently survey large reef areas. Additionally, the intermediate spatial scale of sUAS data can aid in a seamless integration between reef information collection platforms. sUAS data effectively close the spatial gap between traditional remotely sensed and *in situ* reef data. This added layer of information has potential to improve the spatial accuracy of models that aim to predict the future of coral reefs in this changing climate.

sUAS applications are not limited to strict science. Education and public outreach about coral reef issues are necessary in order to inform those outside the coral reef scientific community about important findings and ways they can have direct impacts on coral reef health. sUAS are becoming an essential tool for capturing photography and video of subjects from a new perspective, and can be used to create dynamic, captivating imagery of coral reefs that will increase audience viewership of important coral reef findings and adjacent environmental causes. sUAS can provide a source of entertainment and stimulating education for students interested in various aspects of STEM that range from engineering, aircraft design, mapping to biological applications. Students can work

collaboratively on projects that involve designing, building sUAS, and applying these tools to produce useful, tangible results that can impact their local environment.

Further development of low-cost sUAS that can perform automated flight plans and software capable of cloud based processing and analysis of imagery can enable the integration of citizen science data collection efforts at scales and qualities previously unattainable. The Nature Conservancy (TNC) has applied the use of sUAS to citizen science work to document the impact of an El Niño storm season which brought increased erosion, flooding, and storm damage to the California coastline. "Phones and Drones" connected sUAS users to the flight planning and image processing software Drone Deploy, a cloud-based processing system that uploaded and processed aerial imagery into spatially accurate maps, which in turn were stored and used by TNC to document the impacts of an El Niño storm season. A similar workflow is possible for coastal communities that wish to be more involved with assessing the health of their local reefs. This would allow frequent, community-level coral reef assessments across the globe.

Limitations

Although there are many benefits to incorporating UAS surveys in coral reef science, there are still some limitations that are inherent with remote sensing of benthic habitat through water. Atmospheric radiometric corrections, which are a necessity when processing data collected from satellite and aircraft, are not as important for UAS surveys as there is less atmospheric light scattering between the object and the sensor due to the low altitude platform. However, low altitude remote sensing evokes other issues that must be addressed. As the distance between the sensor and the substrate decreases, water artifacts such as distortions from waves become more pronounced. High frequency waves

such as wind-generated waves (0.1 – 2s periods) are particularly disruptive, inhibiting the collection of accurate spatial data at the colony level, and make benthic classifications challenging. In order to reduce the amount of wind-wave distortions, it is necessary to collect imagery on ultra low-wind days (1-7 KPH) or in protected bays where the fetch is insufficient to produce substantial ripples. Alternatively, Chirayath et al. (2016) introduce a novel mathematical approach that utilizes the magnification distortion produced by wave peaks to magnify the target benthos while eliminating wind-wave distortions[36]. This technique increases the number of possible survey days and locations beyond calm, protected environments, and it increases the spatial resolution over uncorrected imagery 4-10 fold.

Another limitation is the current lack of automated classification systems for high-resolution aerial RGB imagery. Due to the amount of area targeted with sUAS surveys, comprehensive manual benthic classifications are time intensive. Although it is possible to distinguish between live coral and sand, the heterogeneity of both color and morphology within and between coral species makes classifications at the species level challenging when limited to RGB channels. As with standard remote sensing techniques, the use of multi- and hyperspectral sensors on sUAS has potential to vastly improve the efficiency and accuracy of benthic classifications[20].

Spectral imaging cannot only help classify benthic components, but also potentially characterize components within the coral holobiont. Spectral signatures have been used to determine algal pigment concentrations, and this approach is a noninvasive, time-, and cost-efficient technique used to gain accurate pigment concentration values for a large number of samples [21,21,24,45–47]. This technique in combination with sUAS

platforms could potentially determine pigment concentrations of algal symbionts located within the coral host across reefscapes. This information could be used to monitor fine-scale, pre-mortality coral health metrics that can provide new insight to the fine-scale dynamics of coral physiology. There are currently several companies that offer hyperspectral sensors designed for use on sUAS. While prices are still high, advances in technology will continue to make sensors more powerful and cost-effective.

FAA Regulations

Recent strides in technology have increased the accessibility of sUAS for hobbyist, commercial, industrial and, research use alike by decreasing prices and improving usability. The increased presence of sUAS in National Air Space (NAS) has caused the Federal Aviation Administration (FAA) to rethink ~~the~~ regulations on sUAS operations. Previous to May 4, 2016, educational or research use of sUAS was considered commercial operation, which required 333 exemption licenses that were costly and time consuming to obtain, and required the sUAS operator to possess a manned aircraft pilots license (U.S Government Publishing Office: Title 14, Chapter I, subchapter C, Part 45,47,61,91).

The May 4 2016 memorandum clarified that sUAS can be operated under hobbyist rules at educational institutions and community-sponsored events, provided the roperator is not compensated directly or indirectly for operating the aircraft[48]. This ruling primarily focuses on promoting the use of sUAS for STEM education and limits faculty use of the aircraft to "secondary or incidental" to student control. These activities do not require FAA authorization if the aircraft is restricted to several regulations. Some of the more important regulations state that "the aircraft must be operated in a manner that doesn't interfere with and gives ways to any manned aircraft; when flown within 5 miles

of an airport, the operator of the aircraft provides the airport locator and the airport air traffic control tower (when the facility is available) with prior notice of the operations. Operators flying from a permanent location within the 5-mile radius should establish mutually agreed upon operating procedures with the airport operator and airport air traffic controller"[48]. For the fieldwork detailed in this review, a letter of agreement (LOA) between the sUAS operating institution (HIMB) and Marine Corps Base Hawaii (MCBH) was required to conduct sUAS operations, as the targeted reefs are located inside the 5-nautical mile radius of the (MCBH) airspace. Notification protocol for this LOA includes number and model of aircraft, planned flight location, altitude, and time, and real time contact information.

Also important is the standard protocol for the sUAS under lost-link situations and, if possible, modification of the protocol to reduce possible interactions between manned and unmanned aircraft. The sUAS operator must notify the air space controller at least 72 hours prior to planned flight time via email or phone call and must contact the air space controller an hour prior to operations, and again after operations end. For more information on this memorandum and an LOA template, please see supplemental information.

If researchers plan to utilize sUAS for compensated work, a commercial license is required. As of August 29, 2016, the FAA instituted U.S. Government Publishing Office: Title 14, Chapter I, subchapter C, Part 107, which revises the certifications and regulations required for commercial sUAS operations in an effort to further integrate UAS into the NAS[49]. Important points are as follows: 1) Operations are limited to visual line of sight during daylight and civil twilight. 2) Maximum aircraft altitude is 400 ft at

Ground Level (AGL) or within 400 ft of a structure. 3) Aircraft must operate under a maximum speed of 100 mph. 4) The person operating a sUAS must either hold a Remote Pilot Certificate (RPC) with a sUAS rating or be under the direct supervision of a person with a RPC[50]. 5) To qualify for a RPC, a person must "Be at least 16 years old, demonstrate aeronautical knowledge by either passing an aeronautical knowledge test, or hold a part 61 pilot certificate other than a student pilots license, and complete a flight review within the previous 24 months, and complete a sUAS online training course"[50]. While some of these regulations may sound prohibitive, the ruling also states "Most of the restrictions discussed above are waivable if the applicant demonstrates that his or her operation can safely be conducted under the terms of a certificate of waiver." This is especially applicable to coral reef researchers that are planning to operate in restricted airspace over national parks, marine sanctuaries, and within 5 nm of an airport. While the FAA's job is to keep the NAS safe for both manned and unmanned aircraft, sUAS operators should understand that it is possible to waive regulations on a case-by-case basis for operations that will have a low risk of impacting NAS safety.

Conclusion

Considering the very recent introduction of UASs into environmental and conservation sciences, there have been massive advancements of hardware and software that have allowed for the improved efficiency of data acquisition and quality of results. The high degree of versatility of sUAS makes them an ideal tool for reducing costs and increasing time efficiency while producing high-resolution data that has not been possible with previous aerial survey tools. The continued development of high endurance sUAS platforms, accurate autonomous software, and small, powerful sensors, and new, more appropriate airspace regulations will continue to push the boundaries of the amount and

type of information we can collect about coral reefs. The development of efficient, accurate monitoring techniques is a vital component for increasing our ability to understand and protect coral reefs. We believe that sUAS can and will play a major role in providing important information about nuanced coral reef dynamics that will inform management decisions, capture the attention of the general public, and inspire innovation and interest in students about coral reef science.

CHAPTER II

Assessing the spatial distribution of coral bleaching in response to coastal stressors with a low-altitude remote-sensing platform

To be submitted to Coral Reefs

Introduction

Coral reefs are productive, diverse ecosystems that play a vital role in natural and human networks throughout the tropics and subtropics. Coral reefs provide an abundance of physical and biological benefits to coastal economies through tourism, fisheries, and coastal protection[1,51] but are in global decline due to a variety of acute and chronic stressors originating from both natural and anthropogenic sources[52,53]. Natural, local stressors such as sedimentation, nutrient input, and freshwater can have profound effects on reef health[54,55]. Additionally, anthropogenic manipulation of coastal systems through agriculture, river modification, and urban development can degrade local environmental conditions through the chronic, unnatural input of local stressors into coastal waters[56–58]. Chronic exposure to local stressors may result in coral mortality and sub-lethal effects such as disease, altered growth, reduced regeneration, lowered reproduction and recruitment rates, and an overall reduction in reef resilience[59]. Loss of resilience reduces the system's ability to resist and recover from acute events such as severe storms, intense freshwater exposure, or coral bleaching[60]. A chronically stressed reef system is likely to recover slowly, if at all, after an acute event[54]. Faster-growing macroalgae can out-compete the affected coral colonies, which can lead to increased colony mortality, ecosystem degradation and ultimately, regime shifts to a macroalgal dominated system[53,61].

Coral Bleaching

Coral bleaching occurs when a coral is exposed to abnormal environmental conditions and subsequently expels its symbiotic dinoflagellate algae[62,63]. Devoid of symbionts, scleractinian corals have a significantly reduced energy budget, which impairs coral growth, reproduction, capacity to resist disease, and ability to defend against space competitors such as algae[64]. This mechanism increases risk of coral-algal phase shifts, which decreases reef rugosity, and subsequently reduces the biodiversity and ecological capacity of the reef system. Coral bleaching is famously induced by high water temperatures and irradiance[65,66]. Baker et al. (2008) indicate that warm, shallow, low-flow reefs are high-risk locations for coral bleaching, which should predict Kāneʻohe Bay as a likely target for coral bleaching events[62]. However, until recently, coral bleaching has been a historically rare event throughout the Hawaiian Islands, including Kāneʻohe Bay[67].

Study Site

Kāneʻohe Bay, located on the NE side of Oʻahu, Hawaiʻi is the largest sheltered body of water in the main Hawaiian Islands, and is characterized as a shallow, near-shore marine environment with well-developed fringing reefs and 57 distinct patch reefs (Figure 2.1)[68].

Mōkapu Peninsula and a barrier reef create a low-wave energy, low-flow environment punctuated by two deeper channels at the North and Middle/South ends of the bay. While the channels and water-flow over the barrier reef at high tide provide sources of water exchange within the bay, wave forcing is the predominant circulation method for Zones 1-5 (Figure 2.1)[69].

2015 Bleaching event

High irradiance, and subsequent high atmospheric and water temperatures characterize summer months in Kāneʻohe Bay[38,70]. In some instances, low winds coincide with high irradiance to push water temperatures above 30°C, leading to increased potential for coral bleaching[39]. Only three major bleaching events have been documented in Kāneʻohe Bay, with two of the most recent events occurring during consecutive summers of 2014 and 2015. Temperature models confirm that abnormally high sea surface temperature (SST), potentially caused by the Pacific Decadal Oscillation (PDO), was present around Hawaiʻi during these times. The September 2014 event was the most severe bleaching event documented in the Hawaiian Archipelago to date[68]. Bleaching intensity was variable throughout Kāneʻohe Bay, with higher bleaching intensity seen toward the north end of the bay[39]. Coral recovery after the 2014 bleaching event was high within Kāneʻohe Bay, with the exception of reefs affected by a freshwater kill that occurred in July 2014, where recovery has been slow to nonexistent[67]. Widespread coral bleaching was recorded again throughout Kāneʻohe Bay between the months of August and October 2015, again with high recovery throughout the bay (personal communications, Raphael Ritson-Williams, Keisha Bahr).

Water Quality

The Kāneʻohe watershed receives high levels of precipitation and is a highly productive area for agriculture[68]. The fertile nature of the surrounding coastline and the relatively high human populations it has sustained for the past 700 years have subjected Kāneʻohe Bay to a long history of impacts from natural and anthropogenic stressors. The creation of channelized streams has exacerbated the rates and volumes at which coastal runoff enters the bay[71,72]. The impacts of these stressors on Kāneʻohe Bay corals have

been studied extensively[68,73]. Both Hunter & Evans (1995) and Bahr et al. (2015) document how local stressors such as sedimentation, nutrient input, and freshwater have a significant impact on coral health in Kāneʻohe Bay[67,73]. Additionally, studies have shown that polluted conditions have been linked to reduced rates of coral recovery and subsequent overgrowth by benthic competitors after acute events[54,74].

Freshwater Stress

Due to its partially estuarine nature, portions of Kāneʻohe Bay in close proximity to shore may be significantly impacted by seasonal weather patterns. The wet season, which generally runs from October through May, is characterized by lower temperatures, increased rainfall, and higher cloud cover[75]. Prolonged periods of rain and high cloud cover can yield sharp, localized drops in salinity, and have been shown to cause severe, highly localized mortality events on Kāneʻohe Bay patch reefs in close proximity to stream mouths[54,68,73]. In late July 2014, an intense rain event caused a localized drop in salinity to ~15 ppt, which triggered localized mortality on patch reef areas adjacent to point-source outflows[68]. During normal rain events, an increase in coastal runoff volume, which may include a six-fold increase in sediment and nutrient input, can cause physically- and chemically-mediated coral stress[58,76,77]. Therefore, rain events can have numerous possibly synergistic negative impacts on coral health.

Sedimentation

Sedimentation rates can fluctuate drastically in conjunction with precipitation levels. When exposed to high rates of sedimentation, corals produce increased amounts of mucus to facilitate the removal of sediment from the colony surface, known as mucus sloughing. Increased production of mucus reduces energy availability for other functions such as growth, disease defense, and reproduction[26]. Additionally, sediment-smothering

and mucus sloughing reduce the ability of the coral host to absorb dissolved and particulate organic and inorganic nutrients from the water column[27]. Studies have shown that energy expenditure surpasses energy acquisition when sedimentation rates surpass 2000 g m^{-2} day^{-1} [78,79]. Toguchi et al. (1982) estimated that annual sedimentation rates of non-terrestrial particulates in Kāne‘ohe Bay are ~0.49 g m^{-2} day^{-1} [80]. Given that these measurements do not include terrestrial sedimentation rates, it is reasonable to assume that total sedimentation rates on Kāne‘ohe Bay patch reefs are higher than 0.5 g m^{-2} day^{-1}, and may reach 2000 g m^{-2} day^{-1} during heavy storm events. Therefore, the impact of sedimentation, while being a prominent chronic stressor, may only impact reefs at acute time scales. Although sedimentation is known to negatively impact the health of corals, it has been suggested that reduced solar irradiance either via high cloud cover or moderate turbidity from low levels of chronic sedimentation may help prevent severe coral bleaching and improve recovery rates of bleached corals[81,82].

Nutrients

Populated coastal areas produce nutrient-rich runoff that originates from sources such as agricultural and residential fertilizers, septic tanks/cesspools, and freshwater seeps[73]. In a mechanism similar to that of sediment and freshwater transport, nutrient levels in Kāne‘ohe Bay can vary greatly depending on precipitation levels. In periods of consistent or high rainfall, nutrient levels can increase rapidly. High nutrient environments can promote algal growth[67,83], coral disease[84], and bleaching[85]. Additionally, high nutrient environments can reduce coral fecundity, fertilization rates, embryo development[9,86]. Studies have also shown an increase in symbiont density and a reduction in coral growth rates in relation to increased nutrients due to the increased allocation of photosynthetic energy devoted to algal growth instead of host growth[87].

Clearly, nutrient input can be classified as a coastal stressor that impacts reef ecology and coral physiology. Therefore, the added stress associated with the presence of elevated levels of nutrients in a coastal reef system such Kāneʻohe Bay has the potential to impact coral bleaching dynamics. However, similar to the other coastal stressors, levels of nutrients may differ among patch reefs due to the varying physical and anthropogenic forces present in Kāneʻohe Bay.

Local stressors can vary extensively between different sections of Kāneʻohe Bay due to heterogeneous residence times and non-uniform human population distributions[73,88]. Residence times within the bay are defined by six distinct areas in Lowe et al. (Figure 1) [68]. Zones 1 and 4 have low residence times of ~1 day, while Zones 2, 3, and 5 have residence times of ~6, ~3, and ~10 days, respectively[89].

While Zones 1 and 4 have low residence times, the proximity of Zone 4 to the coast, and adjacent stream mouths indicates that reefs in this zone would experience elevated, although temporary, levels of coastal runoff in comparison to Zone 1. Similarly, reefs in Zone 5 should experience higher levels of costal runoff than reefs in Zone 2 or 3, and due to the higher residence times in this zone, Zone 5 patch reefs likely experience elevated coastal stressor conditions for longer periods than Zone 4. However, because Zone 4 receives ~60% of the total freshwater runoff released by Kāneʻohe Bay watersheds, reefs in Zone 4 may be exposed to more extreme runoff conditions than Zone 5 reefs, but on shorter time scales[88].

Low residence times increase the delivery of primary productivity and heterotrophic feeding in addition to enhancing rates of coral tissue recovery as high water flow removes waste products and increases plankton prey availability[90,91]. Given the

heterogeneous nature of flow regimes, and therefore local stressors throughout Kāne‘ohe Bay, it is logical to expect corals in different flow regime zones to experience varying exposure to coastal stressors, therefore eliciting a heterogeneous bleaching response to temperature stress throughout Kāne‘ohe Bay.

Currently, there are no published studies that quantify the spatial distribution of coral bleaching on patch reefs between flow regime areas. This paper aims to explore how the spatial distribution of coral bleaching within and between patch reefs varies in response to coastal stressor gradients, ranging from high exposure to low exposure. This will involve quantifying the spatial distribution of coral bleaching and live coral cover in response to varying levels of nutrients, sedimentation rates, and salinity fluctuations between and within Kāne‘ohe Bay patch reefs during the 2015 coral bleaching event.

In order to investigate this topic, we targeted four patch reefs, each located in a different flow regime zone within Kāne‘ohe Bay. Patch Reefs 44, and 25 are located in Zones 4 and 5 respectively and are designed to represent reefs that are exposed to higher levels of coastal stressors. Although there are no patch reefs located in Zones 1 or 2, Reefs 42 and 20 are located on the “buffer zones” between 4 and 1, and 5 and 3 respectively, and should offer contrasting environmental conditions to Reefs 44 and 25 while minimizing distances between reefs (Figure 2.1). Each of the four reefs has varying sizes and estimated coral cover (Table 2.1). It is important to note that for over 30 years, introduced *Kappaphycus/Eucheuma* macroalgae dominated many patch reefs in Kāne‘ohe Bay, including Reef 44[92]. Out of the targeted reefs, only Reef 44 experienced significant algal cover until the 2014 freshwater kill in caused mass mortality of coral, algae, fish, and invertebrates on portions of the reef[67]. Over the past year, Reef 20 has

experienced colony-wide protein losing cytopathology, which impacted four reefs adjacent to and south of the sandbar in mid-bay[93]. The disease was first documented early February and last seen in late March 2015. It is important to note that this reef is adjacent to a sandbar region that is a popular recreation destination for ~~many~~ boaters. Several boat scars have been documented on this reef, and it is not uncommon for boaters to leave trash and other pollutants in the area.

Coral Bleaching Survey Techniques

Current *in situ* reef survey methodologies are time, money, and labor-intensive, making regular surveys of large reef areas unfeasible. While *in situ* surveys are important for collecting single animal or colony information, these methods usually collect categorical data, which are ineffective for understanding fine-scale spatial dynamics in a larger context. Additionally, reef community structure is extremely heterogeneous over scales of centimeters to hundreds of meters[13]. Therefore, conducting an *in situ* assessment of a sample reef population is not necessarily be an accurate representation of the reef as a whole, which poses a problem for a study that requires detailed colony-level information across a large reef area.

Remote sensing methods such as satellite imagery have contributed enormously to the characterization of coral reefs by providing otherwise unattainable large-scale reef information[26]. However, traditional remote sensing methods produce relatively low-resolution images that do not provide sufficient colony-resolution data. Additionally, satellite and airborne data collection require an immense amount of planning, funding, time, and good fortune in order to collect clear images that are not obscured by atmospheric noise and water column turbidity.

While *in situ* and remote sensing techniques may be used to collect reef information at the two ends of the spatial spectrum, another methodology must be utilized to collect intermediate-scale reef information that captures colony- level information within the full-reef context . In order to obtain high resolution, large-scale reef data, aerial information must be collected at lower altitudes

The recent production of commercial UASs (Unmanned Aerial Systems) has already begun to revolutionize the way scientists conduct conservation biology research. This technology provides an important middle ground between *in situ* and traditional aerial imaging methodologies, collecting high-resolution, continuous data that can observe coral reef dynamics at the colony level. UASs are cost effective (<US $2000), transportable, require minimal assembly, carry small, powerful sensors, and fly at low altitudes with a high degree of control under autonomous flight. UASs offer a viable alternative to traditional platforms for acquiring high-resolution remote-sensing data at lower cost, increased operational flexibility, and greater versatility. Small UASs (sUAS) are defined as fixed wing or multi-rotor aircraft that weigh less than 25 kg. and are flown without a pilot in the cockpit[29,30].

sUAS are currently used for various conservation studies such as wildlife surveys, wetland assessments, and coastal erosion assessments[30,33–35]. This innovative technology is still mostly unexplored in the field of coral reef ecology, and presents a unique opportunity to redefine the tools commonly used for shallow-water benthic studies. We utilized this technology to assess percent live, bleached, and paling coral cover of large areas of Kāneʻohe Bay patch reefs.

Methods

At the time of preparing for this project in early 2015, there were limited options for low-cost, commercially available multi-rotor sUAS. The DJI Phantom 2 was a suitable platform because it had a flight time of over 15 minutes, could hold a 3-dimensional gimbal and 12 megapixel (MP) RGB sensor, and had flight-planner capabilities. The 3-dimensional gimbal keeps the camera level on three axes, allowing for smooth, stable, imagery collection regardless of the pitch and yaw of the moving platform. A GoPro Hero 3 was a suitable RGB sensor due to its small size, light weight, and capability to collect 12 MP images. The GoPro was fitted with a circular polarizer to reduce glare artifacts as much as possible. DJI produced a free, compatible flight planner for iOS or Android tablets that enabled the pilot to create up to 16 waypoints per flight on a satellite map-layer interface. Waypoints could be manually adjusted for location, height, time spent at waypoint, platform orientation, and speed between waypoints.

Using this array of hardware and software, we collected individual, overlapping aerial images of each patch reef at an altitude of 15-20 m. Maximum flight time for the DJI Phantom 2 was ~15 minutes per battery. Due to this constraint, the UAV was programmed to fly at 5 m s^{-1}, which resulted in full reef coverage requiring between 0.5 and 5 batteries, depending on reef size.

Pre-flight procedure

Prior to conducting the UAS assessment, it was important to establish ground control points (GCPs) in order to obtain accurate geospatial information for post processing steps. Five floats and four L-shaped PVC pipes were distributed across the reef periphery. The floats and PVC pipes were used as the GCPs and were easily visible from the UAS. The PVC pipes were 0.34 m × 0.34 m with red, green, and blue tape on

each arm for colorimetric and additional scale calibrations. GPS coordinates of the GCPs were recorded with a recreational-grade GPS unit (Garmin GPSMap 76cx) and were used for georeferencing the orthomosaics during post processing.

Flight Operations

All four UAS reef assessments were conducted from the bow of a 17-ft Boston Whaler between 0830 and 1000 hrs. (HST). Early-morning flights were desired to reduce glare hot spots produced by direct overhead sunlight. The boat was anchored on the leeward side of each reef during UAS operations. The pilot launched the aircraft while the spotter initiated the flight plan on the tablet. The waypoints were programmed in a lawn-mower pattern, allowing the sensor to travel over the reef, collecting still imagery at sufficient overlap in the x and y direction for the post processing mosaicking workflow. The GoPro Hero 3 sensor had a field-of-view of 94° and 120° in the x and y direction respectively, in the "Wide" setting, and at 20 m altitude, the flight paths needed to be 15-20 m apart, traveling at a maximum of 5 m s^{-1} in order to collect sufficient overlap in the x and y direction. The pilot visually monitored the aircraft while holding the remote control and the spotter assessed flight progress with the tablet. When the survey lines were completed, the pilot regained manual control and brought the aircraft to the bow of the boat to be retrieved by the spotter. Before each flight, the proper authorities at Marine Corps Base Hawaii (MCBH) and Honolulu International Airport were notified of flight locations, platform, and time of flights in accordance with current FAA rulings at the time.

Partial to complete areas of each targeted patch reef were collected during the bleaching event. Due to weather conditions, the ability to collect imagery of all reefs within a short time span was not possible. Imagery for Reef 44 was collected on August

23, 2015, while imagery for Reefs 42, 25 and 20 was collected between October 27 and October 29, 2015.

Environmental Parameters

Water quality data were collected from single permanent stations on each of the four patch reefs. ~100 ml of surface water were collected within 5 m of each permanent station using 250 cc narrow-mouth Nalgene plastic bottles. Samples were collected at each reef every 2-3 weeks throughout the bleaching period of August to October. Samples were frozen for later phosphate and salinity analysis, and weather anomalies that could significantly impact water quality were recorded.

Phosphate concentrations for each water sample (n=32) was determined using the molybdenum blue method as per Strickland & Parsons[94]. Salinity measurements for each water sample were conducted using an YSI 85: O_2, Conductivity, Temperature and Salinity sensor with an accuracy of 0.01. Sediment traps were constructed of PVC pipes of uniform size, were capped on one end, secured to the permanent station at a depth of ~2 m at each reef, and oriented so the opening was parallel to the water surface. PVC pipes were recovered and replaced every month. After removing organisms within the pipes with a coffee filter, the sediment was filtered using 0.2μm filter paper. The weight of the dried, filtered sediment was divided by the deployment days to determine an average daily sedimentation rate.

In order to understand within-reef variation in coastal stressors, three additional sediment traps were deployed on opposite edges of each reef for a 30-day period. These sedimentation rates were used as a proxy to provide preliminary information about within-reef variability of coastal stressors as we assume sedimentation rate is relatively connected to coastal salinity and nutrient concentration.

Analysis

Image processing

After collecting the still RBG imagery, Adobe Lightroom was used to remove unnecessary images, calibrate images to remove wide-angle distortion, and standardize color between images. The single images were combined into mosaics using Agisoft Photoscan, which uses SfM algorithms to combine adjacent images within a scene to create orthomosaic models of a complete patch reef[40]. This is a cost-effective, computationally efficient technique that has been used successfully in various terrestrial aerial, and marine in-situ photogrammetry studies to produce accurate 3-D models of targeted substrate[40–42,95]. It is important to note that in order to produce high quality mosaics, SfM software generally requires a minimum of 60% overlap between single images in both the vertical and horizontal axis. This overlap is especially important if the images are not geo-tagged, and therefore cannot be positioned using image-specific GPS information. ArcMap was used to geo-reference each image mosaic to a map coordinate system using GPS information collected for the GCPs.

Ground Truthing

In situ ground-truthing was performed to evaluate the quality of the airborne imagery, utilizing both 1 m × 1 m photo-quadrats and 10-m-long photo-transects. The *in situ* photographs were not used for rigorous, statistical accuracy assessment, but rather for qualitative comparisons that highlighted the airborne imagery's ability to resolve different benthic types (Figures 2.2-2.4).

Image Classification

Initially, we attempted to use automated classification schemes in ENVI and ArcMap, but due to the heterogeneity of color and shape of the coral species present,

classification results were not consistently accurate between reefs. Additionally, sand and bleached coral have similar reflectance values due to their similar "brightness" values from a 3-band, RGB sensor. Therefore using a color-dependent classification scheme did not prove suitable for differentiating between sand and bleached coral.

Ultimately, image annotations were conducted manually in ArcMap. The polygon outline of each coral colony was digitized by hand and assigned one of three health states: paled, bleached, and full pigmented which we will refer to as "healthy". Three Shapefiles were created, including one to store the polygons for each coral health state. Non-coral cover such a sand, rubble, and algae was not specifically cataloged, as these metrics were not relevant to the study.

Spatial and Statistical Analysis

To calculate coral cover metrics, all polygons for a given health state were dissolved into a single large polygon that contained all areas of that health state. This produced a total of three polygons; one each for bleached, paled, and fully pigmented coral. The area of each of these polygons was divided by total reef area to determine proportional cover for each coral heath state, as well as total coral cover per reef.

A point layer of each individual polygon was created to conduct cluster analyses. We used the Spatial Autocorrelation Moran's I tool within the Spatial Statistics toolbox to determine the spatial pattern of each health state on each reef. We then used the Optimized Hot Spot Analysis tool in the spatial statistics toolbox to determine the location of high and low clumped areas of each health state on each reef (Figure 2.11 c & d 2.12 c & d, 2.13 c & d. 2.14 c & d).

Statistical analysis of the environmental data was conducted using R v3.3.2 (R Core Team 2015). A Kruskal-Wallace test was used to assess differences of each

environmental stressor (salinity, sedimentation rates, phosphate concentration) between reefs. A linear mixed effects model (package lmerTest, Kuznetsova et al. 2015) was employed to identify which reefs have significantly different PO_4 concentrations, as well as the magnitudes of the differences[96]. A 2-way ANOVA was used to assess differences in sedimentation rates within each reef. Beta regression analysis was used to determine relationships between coastal stressors and unhealthy coral cover using all environmental data time points, and isolating time points collected just before the sUAS surveys[97]. ENN metrics in FRAGSTATS (version 4.2) were used to determine spatial patterns between bleached, paled, and healthy coral colonies. Euclidean nearest neighbor (ENN) value is the distance (m) to the nearest neighboring patch of the same type and is based on shortest distance from cell center to cell center[98].

Results

Between-Reef Environmental Variability

A Kruskal-Wallace test for non-normal distributions showed phosphate is the only coastal stressor out of the three tested that significantly differed between reefs ($p < 0.05$). Pairwise comparisons revealed that phosphate values on Reef 44 were significantly higher than on Reefs 20 and 42 ($p < 0.05$ for both) by 62 and 42 nM respectively (Figure 2.5). Though not statistically significant, Reef 44 had the largest variance in salinity, but not the lowest recorded value. Reefs 42 and 44 both had instances of very low salinity (<20 PPT). Daily mean temperatures from January to October 2015 varied significantly between all reefs except for Reefs 25 and 44[99]. However, due to the high sample size (n=901), pairwise tests show the average significant temperature variation between reefs as 0.0115°C, which is smaller than the accuracy range for the temperature logger (±0.53°C). Therefore, we considered temperature as constant between reefs for the

purposes of this study.

Within-Reef Variability

A 2-way ANOVA showed sedimentation rates did not differ significantly within each reef. The low variance of sedimentation rates at sites within Reef 20 signified relatively uniform sedimentation conditions throughout the reef while Reefs 42 and 44 had larger variations between sites within each reef (Figure 2.6).

Coral Health

Coral health was originally categorized into three classes (bleached, paled, fully pigmented). However, for the stressor/coral cover analysis, coral health was reorganized into two categories (healthy and unhealthy) in order to maintain legitimate comparisons between reefs, as the Reef 25 date set lacked paled coral. Percent cover of unhealthy or healthy coral was not significantly correlated to the standard deviations of any coastal stressors (Figure 2.7). Percent covers of unhealthy and healthy coral were both significantly correlated with mean salinity ($p < 0.05$) and mean phosphate ($p < 0.05$) (Figure 2.8.

Time Lags

Salinity values collected right before the reef imagery were highly correlated with percent unhealthy coral cover ($p < 0.05$, $R^2 = 0.9811$) (Figure 2.9).

Spatial Statistics

All reefs were classified as significantly clumped using Moran's I spatial autocorrelation test (Table 3). ENN values differed significantly between reef ($\chi 2 = 399.68$, $df = 3$, $p < 0.001$) and health type ($\chi 2 = 1115.2$, $df = 2$, $p < 0.001$). Variance between bleached ENN was visibly larger than healthy or paled, while there were minimal visible differences in ENN variances between reefs. Note the large tails on each

of the plots (Figure 2.11). The highest mean ENN values were found on bleached colonies at Reefs 20 and 42 while the lowest mean ENN values were found on healthy colonies at Reef 20. Reef 42 had the overall highest mean ENN values while Reef 20 had the lowest (Table 2.4).

Discussion

Coastal Stressors

While assessing stressor variation between reefs, we determined that Reefs 42 and 20 were exposed to significantly lower PO_4 concentrations than Reef 44 (Figure 2.5). Considering Reefs 44 and 42 are located in high flow regimes while Reef 25 is located in the low flow regime, these results indicate possible finer-scale environmental differences that separate the 'further from shore' reefs (Reefs 20, 42) from the 'closer to shore' reef environment (Reefs 44, 25). However, the vast ranges in salinity, specifically the spikes of low concentrations on Reefs 42 and 44 (17.6 - 33.0, and 19.1 -33.1 ppt, respectively), indicate this environmental forcing can impact both 'closer to shore' and 'further from shore' reefs in this study[54].

There was no significant variability in sedimentation rate within each reef (Figure 2.6). Although statistically insignificant, Reef 20 had-visibly smaller variance between blocks (Figure 2.6), and insignificance may be the result of a small sample size. If so, Reef 20 may experience possible reef-wide heterogeneous exposure to other coastal stressors in comparison to other reefs in this study. This finding could be due to small reef size and close proximity to the fine-grained, sediment-rich sandbar, which could deposit low amounts of sediment across the reef during discrete high wind/wave events.

Additionally, large variations and higher sedimentation rates within reefs were found on Reefs 44 and 42 (Figure 2.6). This result is encouraging considering the relative

large size of these two reefs would suggest that there should be some environmental variability within each reef. However, it also indicates that there may be two possible sediment sources. A reef further from shore such as Reef 42 can potentially experience this much sedimentation due to its close proximity to the sandbar, while Reef 44 accumulates terrestrial sediment from the plume created by Kaʻalaea Stream. Based on this evidence, it would be useful to analyze sediment composition to gain an accurate view of fine-scale sedimentation dynamics within Kāneʻohe Bay. Additionally, there are some caveats to these results. Sediment data from non-permanent locations (b, c, d) were collected for a single, different month for each reef (Figures 2.11 c & d, 2.12 c & d, 2.13 c, 2.14 c & d). While the permanent block (block a), which was collected for all reefs at the same time reduces this issue, variations in sedimentation rate between reefs could be an artifact of different environmental conditions between sampling months. For instance, an intense rain event during the collection month for Reef 42 may have produced a spike in sedimentation rates, while the lack of heavy rain events during the collection month for Reef 20 could have produced subdued sedimentation rates and a smaller variance (Figure 2.6).

Survey Methodology Comparison

A variety of survey methods are currently used to collect reef data, and estimating coral cover based on a small survey areas risks inaccuracies due to the heterogeneous nature of coral reefs[12]. The State of Hawaiʻi Division of Aquatic Resources (DAR) conducted a full assessment of Kaneohe Bay patch reefs in 2014 using *in situ* "snap assessment" techniques[39]. The snap assessment method, as described in Neilson et al. 2014, collects coral cover observations across a large portion of reef area[39]. Although the DAR data were collected ~1.5 years prior to these sUAS surveys, the earlier data sets still

provide an interesting comparison between survey methods. The largest discrepancies in coral cover are between Reefs 25 and 20 (Table 2.5). Reef 25 is overrepresented by *in situ* surveys while Reef 20 is underrepresented. The discrepancy in Reef 25 coral cover values may be the result of high coral cover along the reef edge, which is difficult to capture via aerial imagery, and large rubble and sand patches across the shallow reef flat, which is mostly inaccessible to snorkelers (Figure 2.12 a & b). Alternatively, Reef 20, which is deeper, has a smaller sand patch on the reef flat and lower coral cover on the reef edge (Figure 2.11 a & b). It is also important to note that although the sUAS data are spatially continuous, some of the surveys did not cover complete reef areas. Noting this, it is interesting that the most similar coral cover values between *in situ* and airborne methodologies occurred on Reef 44, which has the largest area and has the lowest percent reef cover collected by sUAS surveys (Tables 2.1, 2.2). Further work could help determine the optimal reef survey area to increase coral cover accuracy with *in situ* methods.

Coral Health Response to Coastal Stressors

Variance in stressor levels does not explain differences in unhealthy or healthy coral cover between reefs, while mean salinity and phosphate concentrations are both significantly correlated to healthy and unhealthy coral cover (Figures 2.7, 2.8). The strong, negative relationship between mean salinity and percent unhealthy coral cover (Figure 2.8 d) supports previous work showing that exposure to low salinity conditions decreases coral resilience to thermal stress[100]. Mean phosphate concentrations, which were used as a proxy for general nutrient stress, have a positive relationship with unhealthy coral cover (Figure 2.8 f). This supports other work that documents the negative impacts of nutrients (specifically phosphate) on thermal tolerance, prevalence of

disease, and early life history of corals[55,85,101]. Additionally, higher nutrient environments promote increased algal biomass and therefore coral-algal competition[87,102]. This can be demonstrated on Reef 44, which had significantly higher phosphate concentrations than two of the 'further from shore' reefs, had at least double the percent algal cover than the three other reefs until a recent freshwater event[39,67].

When assessing the environmental conditions in close temporal proximity to image collection, salinity has a strong negative correlation with cover of unhealthy coral (Figure 2.9). Apart from confirming previous results, the fact that short-term phosphate concentrations do not significantly influence unhealthy coral cover brings up interesting points. From a biological perspective, these results could be supported by conclusions from previous studies that document the impact of nutrient stress as chronic rather than acute[52]. Because salinity can be considered an acute stressor, it could show up as having a more significant impact on coral health on shorter time scales than nutrients[67, 62]. However, it should be noted that since salinity and phosphate data for this project were collected from surface water and surface water quality values can be highly variable, these values may not be representative of generalized, reef-wide environmental conditions at the coral-water interface[88]. While it is important to consider the high variability of surface water measurements at small temporal and spatial scales, these results could be showing important trends of temporal significance to coastal stressor-coral health dynamics.

Spatial Analysis

While autocorrelation tests showed significantly clumped distributions for all reefs (Table 2.3), Reef 44 had the highest Z score, which signifies the most clustering of health types. This result is probably a product of several reef traits. First, Reef 44 has the

highest proportion of unhealthy (paled and bleached) coral (Table 2.2). Due to the inherent heterogeneity of color and texture between and within Kāne‘ohe Bay coral colonies, it is harder to visually isolate individual healthy colonies than those that are paled or bleached. This yields a bias towards higher clumping values of paled and bleached coral, and less for healthy coral. Second, missing reef imagery (Figure 2.14) might produce an artificial clumping phenomenon between the two sections of reef that were actually imaged. Third, the larger reef size translates to a relatively small search threshold, which could also introduce artificial clustering artifacts, although it should be noted that the search threshold is determined automatically by the spatial autocorrelation analysis.

ENN values were highly significantly different between both health type and reef (Figure 2.10). Bleached colonies had the largest mean distances between patches with highest values on Reefs 20 and 42 (Table 2.4). This is an interesting finding considering the high coral cover and healthy percent cover on each of these reefs. It would lead us to believe that on ‘healthier’ reefs, unhealthy coral is slightly more dispersed across the reef instead of clumped in specific areas. However, considering the vast number of outliers for each plot, the results could be an artifact of oversampling due to the high number of patches used for this analysis (n = 16,522).

General Conclusions

The environmental analyses showed that exposure to nutrients are significantly higher on ‘closer to shore’ reefs than ‘further from shore’ reefs, which supports the idea that environmental factors vary at smaller spatial scales than flow regime zones (Figure 2.1). Both phosphate and salinity were significantly correlated with unhealthy coral cover, while only salinity was significant when looking at environmental data collected

just before coral data collection. This may show chronic phosphate presence and acute salinity stress promote increased coral bleaching cover during periods of uniform elevated temperature.

A combination of several stressors is known to exert interactive effects on coral reefs, and promote a chronic decrease in coral resistance to acute stressors such as temperature[52]. In this case, it is possible that the acute influence of salinity compounded the stress caused by chronic nutrient exposure at Reef 44, resulting in increased bleaching and paling cover. Sedimentation rates did not prove to be a significant factor in this study. Average sedimentation at reef sites was higher than those found by Toguchi (1982) (~6 g m^{-2} day^{-1} vs. ~0.5 g m^{-2} day^{-1}, respectively)[33]. However these sedimentation values are much lower than the 2000 g m^{-2} day^{-1} threshold that signifies the point where energy expenditure surpasses energy acquisition, which supports the lack of significance between sediment stress and unhealthy coral cover in this study[31, 32]. Alternatively, sediments can act as a nutrient source[103]. Therefore, it is possible that the higher sedimentation rates found on Reef 44 (which theoretically come from terrestrial origins) could be another potential nutrient input, impacting coral health in ways unseen by analysis performed in this study. Further sediment composition analysis is required to verify this idea.

Limitations

While assessing the results discussed above, it is important to understand and address the limitations of this study. Due to logistical and airspace issues explained below, reef imagery was collected at inconsistent time points. Imagery for Reef 44 was collected on 23 August 2015 while imagery for Reefs 42, 25, and 20 was collected on October 29 & 30. While it is possible for bleaching cover to change dramatically within

two months, coral bleaching in Kāneʻohe Bay mostly peaked at the end of August and remained constant before recovery started at the beginning of November (personal communication, Raphael Ritson-Williams). Imagery we collected of Reef 25 during August and October confirmed that, at least on Reef 25, there was no recovery between August and end of October, but rather a possible slight increase in bleaching cover. If we were to assume a similar bleaching/recovery trend for all four reefs, Reef 44, which already had the highest unhealthy coral cover in August, would be expected to have similar if not higher unhealthy coral cover in October. This would only strengthen the trends between coral health and environmental stressors found in this study, and therefore the temporal inconsistency in data collection does not substantially impact the studies' outcome.

An important part of assessing coral health during a bleaching event is monitoring bleaching recovery. For this study, we collected imagery that represents single time points for each targeted reef. While this gives us an accurate snapshot of coral health during each survey, we do not have any information about rate of bleaching or recovery of all reefs. If possible, an ideal sampling strategy would have been to collect reef imagery on a monthly basis from May (one month before bleaching) through to January (after full bleaching recovery). This would have allowed us to follow fine-scale temporal and spatial bleaching dynamics across four reefs from healthy, to paling and bleaching through to post- recovery. Hindsight is 20:20.

Due to the small number of reefs sampled (n = 4) in this study, it is dubious to draw any firm conclusions from the coral health -environmental stressor analyses. Ideally, we would have included two more reefs located in south bay, which inhabit Zone

6 of the flow regime figure (Figure 2.1). Adding coral and environmental data from additional reefs would help increase the sample size to help us produce more concrete patterns of bleaching-coastal stressor dynamics. However, routine collections of environmental stressor data are time intensive. Additionally, since salinity and phosphate data are collected from surface water samples, increasing sampling locations may introduce more noise than useful data. To conduct a proper assessment of environmental stressor presence per reef, semi-permanent/permanent sensors located at reef-depth are required to collect continuous sedimentation rates, and phosphate and salinity concentrations at each reef. Unfortunately this technology is still not commercially available for phosphate sensors, and salinity sensors of this type are still prohibitively expensive for most studies.

Increasing the number of target reefs surveyed is feasible with minimal effort due to the efficiency of sUAS surveys. However, there were other issues that prevented the inclusion of additional reefs. First, laws regarding sUAS operations within airport airspace were in flux, and the personnel we were required to contact before flights changed after our initial surveys. It took several months to develop a letter of agreement between Marine Corps Base Hawaii (MCBH) and the Hawaii Institute of Marine Biology (HIMB) in order to legally conduct sUAS operations in MCBH airspace under the new educational operations clause created by the FAA (Levy et al. in review). Also, weather limits "flyable" days and substantially restricts the amount of time per day to collect clear imagery (Levy et al. in review). Additionally, the current process used to classify reef imagery at a colony scale is extremely time intensive. Therefore, post-processing time and manpower availability is an important factor to consider when planning future sUAS

surveys.

The goal of utilizing sUAS to collect coral bleaching data was to get a comprehensive view of bleaching across entire patch reefs. However, due to inefficiencies inherent to the earlier sUAS used, it was challenging to acquire complete coverage of the larger patch reefs (Table 2.1, Figure 2.14). At the time of conducting these surveys, the UAV platform had a flight time of ~ 15 minutes, and a ground station that created inefficient flight paths that did not always provide sufficient overlap for structure from motion photogrammetry. While it was possible to exchange batteries between flights, larger reefs required more batteries that we had available. Additionally, the DJI 2 platform and GoPro Hero 3 sensor did not create geo-tagged images, which improve the accuracy and completeness. Current systems have longer flight times, more efficient, flight planners and geotagging capabilities that have dramatically increased the quality and range capabilities of sUAS surveys (Levy et al. in review).

Conclusion

Despite these limitations, spatial results from this study have provided a unique, comprehensive understanding of the extent, and distribution of bleached, paled, and healthy coral on four Kāneʻohe Bay patch reefs during the 2015 global coral-bleaching event. Environmental stressor analysis begins to investigate how the combination of chronic and acute stressors erodes coral resistance to thermal stress, which significantly impacts coral bleaching dynamics throughout the bay. However, due to the limitations identified here, this work highlights the need for further investigation into the impacts of coastal stressors and water flow on the health of Kāneʻohe Bay corals. Ultimately, this project has provided valuable insight into the relationships between Kāneʻohe Bay patch

reefs and coastal stressors at previously unexplored spatial scales, and demonstrates the effective use of sUAS surveys in the field of coral reef science.

TABLES

Table 2.1. Patch reef area and coral cover. Excerpt from Nielson et al [23].

Reef	Area (m^2)	Estimated Coral Cover (%)
44	47,068	33
42	17,693	49
25	23,331	24
20	1,855	46

Table 2.2. Coral health categorized into percent healthy, unhealthy, and total coral cover by reef.

Reef	Unhealthy (%)	Healthy (%)	Total Coral Cover (%)	Total Reef Cover (%)
20	2.187000	97.77181	54.968349	100
25	6.905260	93.09474	9.606696	78.5
42	3.705461	96.29454	56.033920	94
44	45.430007	54.56999	32.028950	52

Table 2.3. Z-scores and search thresholds of Moran's I spatial autocorrelation test.

Reef	Z-Score	Search Threshold (m)
20	35.172	3.645
25	31.506	9.805
42	37.379	6.198
44	65.684	3.721

Table 2.4. Mean patch ENN values by reef and coral health. Standout values are bolded.

	Bleached	Healthy	Paled	Average
20	**1.36**	**0.22**	0.49	**0.42**
25	0.94	0.40	NA	0.73
42	**1.70**	0.34	1.11	**0.90**
44	0.87	0.41	0.40	0.48
Average	**1.01**	**0.38**	0.52	

Table 2.5. Patch reef coral cover comparing *in situ* and sUAS survey techniques. *In situ* data was collected by DAR from February-April, 2014 [23]. sUAS data was collected from August-October 2015. Amount overestimated by *in situ* method is underlined.

Reef	Total Coral Cover (%) (sUAS)	Estimated Coral Cover (%) (*In situ)*	Difference
44	32.03	33	<u>0.97</u>
42	56.03	49	7.03
25	9.61	24	<u>14.39</u>
20	54.97	46	8.97

FIGURES

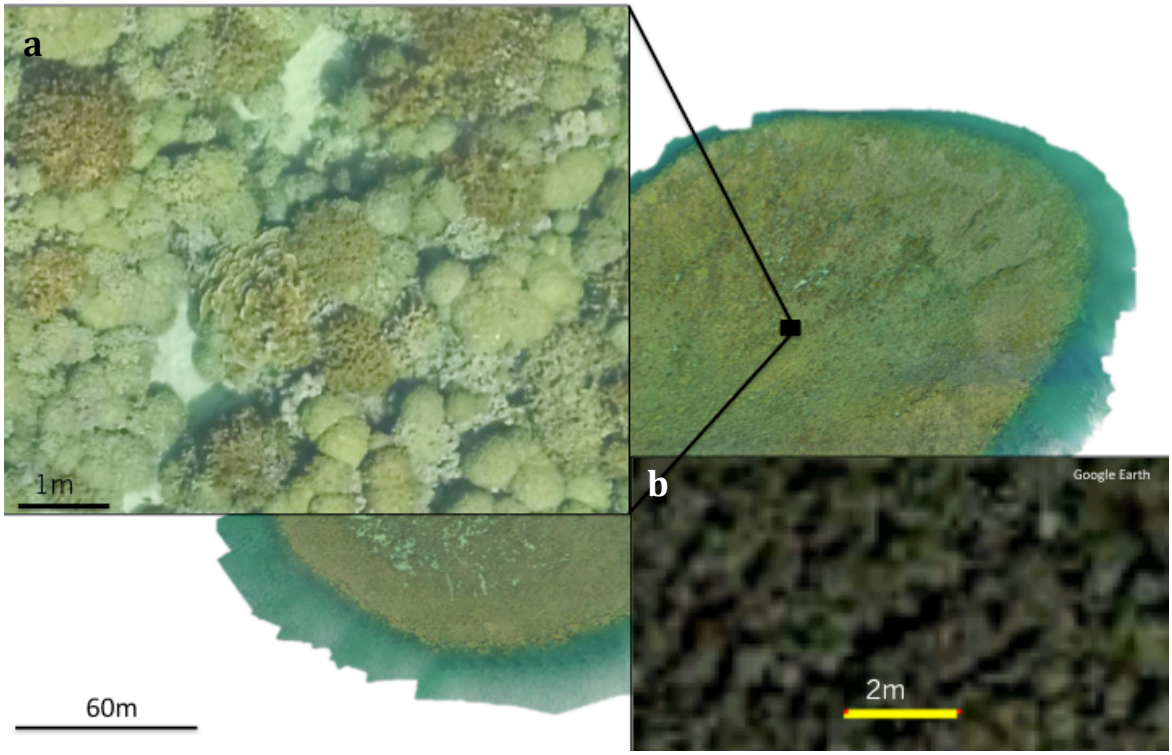

Figure 1.1. UAS survey of Kaneohe Bay Patch Reef 44 at 20 m altitude on 1/20/2015. Total reef area 47,000 m^2. a) 35 m^2 subset demonstrating colony-level resolution. b) Satellite imagery of same reef area.

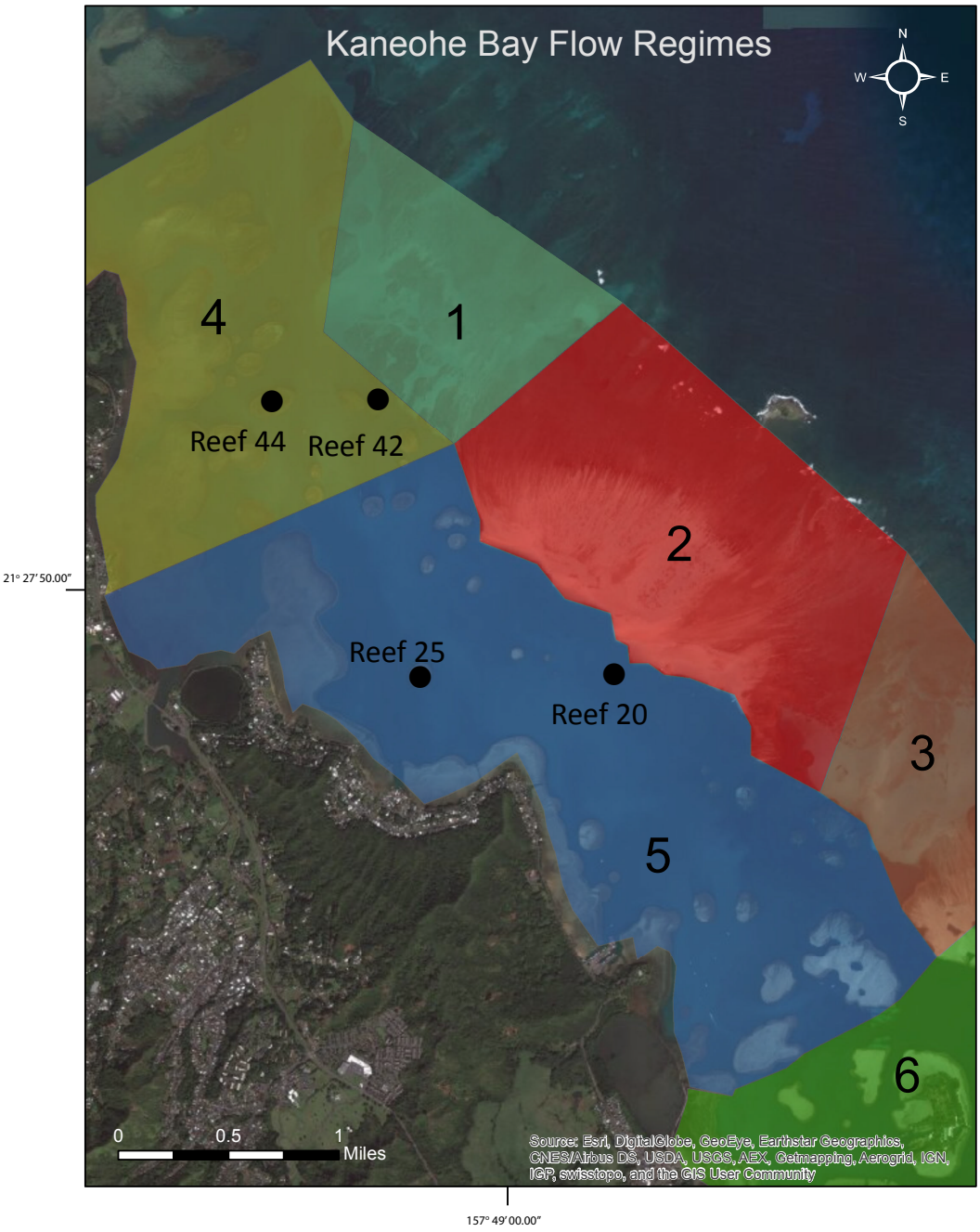

Figure 2.1. Kāneʻohe Bay satellite imagery with an overlay of associated flow regime areas as described by Lowe et al. 2009. The four patch reefs targeted in this study are highlighted.

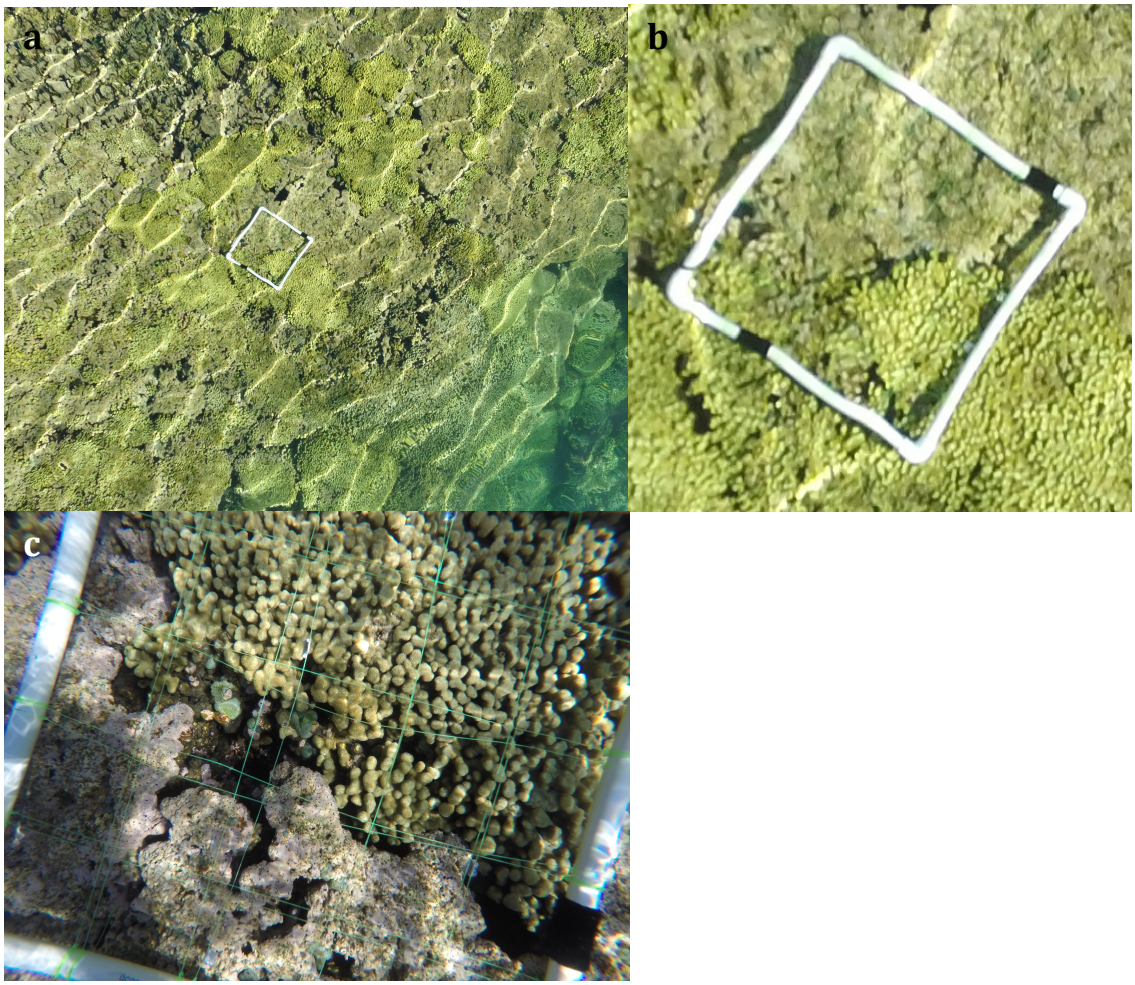

Figure 2.2 Ground-truth verification of aerial imagery. a) Aerial Image taken of healthy coral and non-coral substrate inside the $1m^2$ quadrat at 20 m altitude. b) Cropped aerial image to isolate the quadrat. c. *In situ* imagery of the quadrat. Note the insufficient image coverage of the *in situ* quadrat due to shallow reef depth.

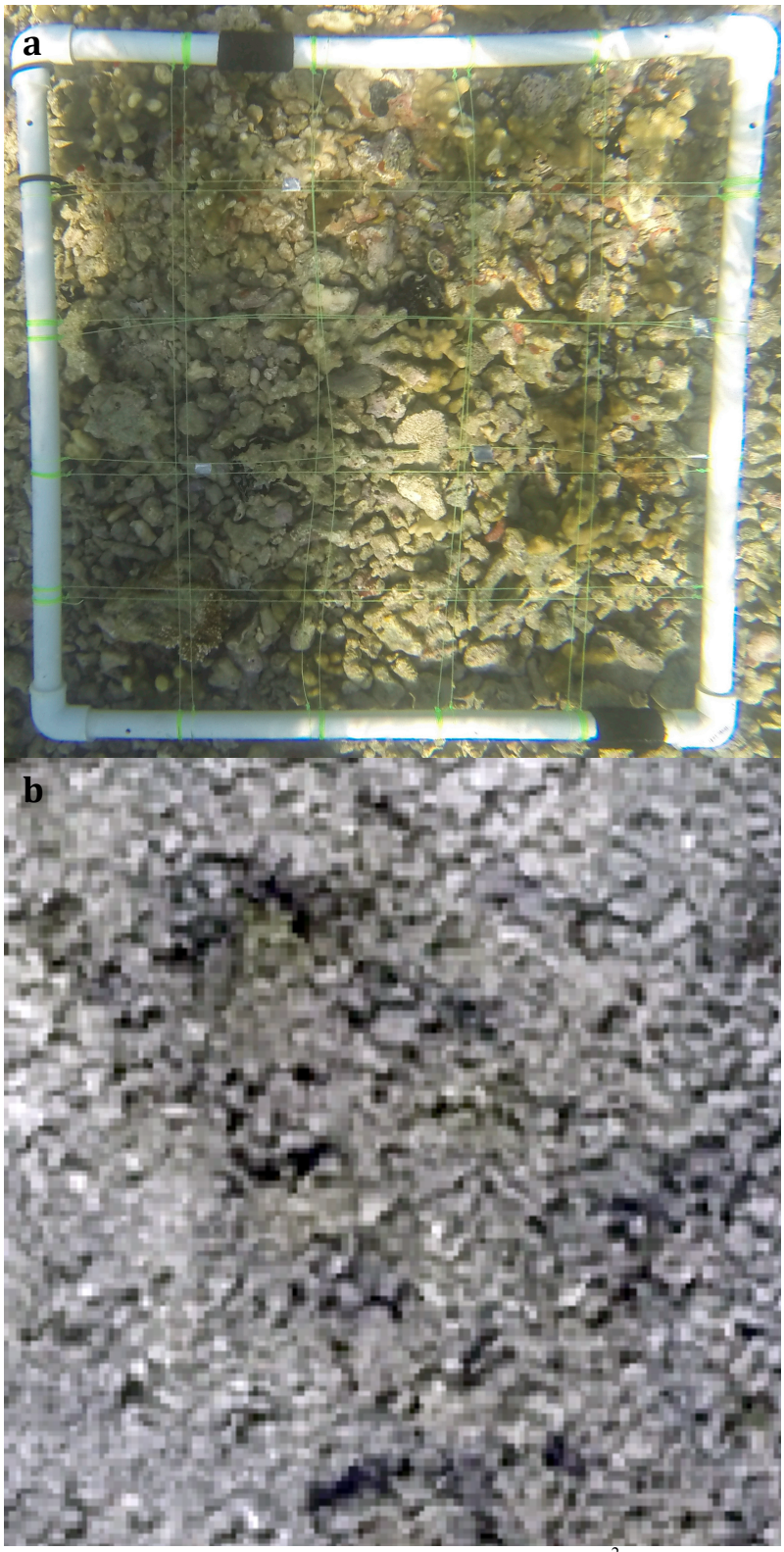

Figure 2.3. Example of rubble/non-coral substrate. a) 1 m^2 *in situ* quadrat. b) 1 m^2 crop of aerial imagery

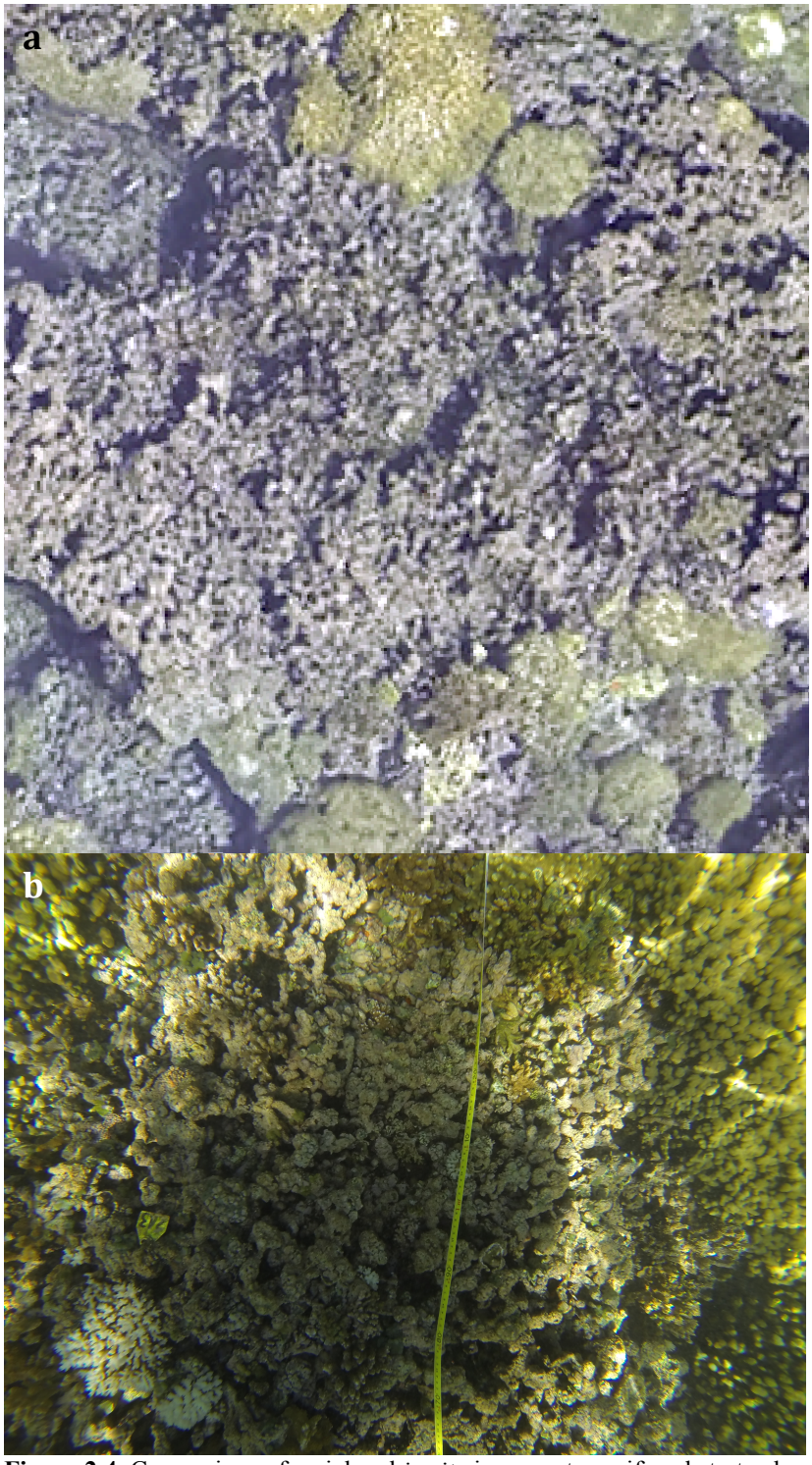

Figure 2.4. Comparison of aerial and *in situ* imagery to verify substrate class. a) Aerial image taken from 20 m of healthy coral (top right) and dead coral/non-coral substrate (center). b) *In situ* imagery of the healthy coral and dead coral/non-coral substrate under the transect line.

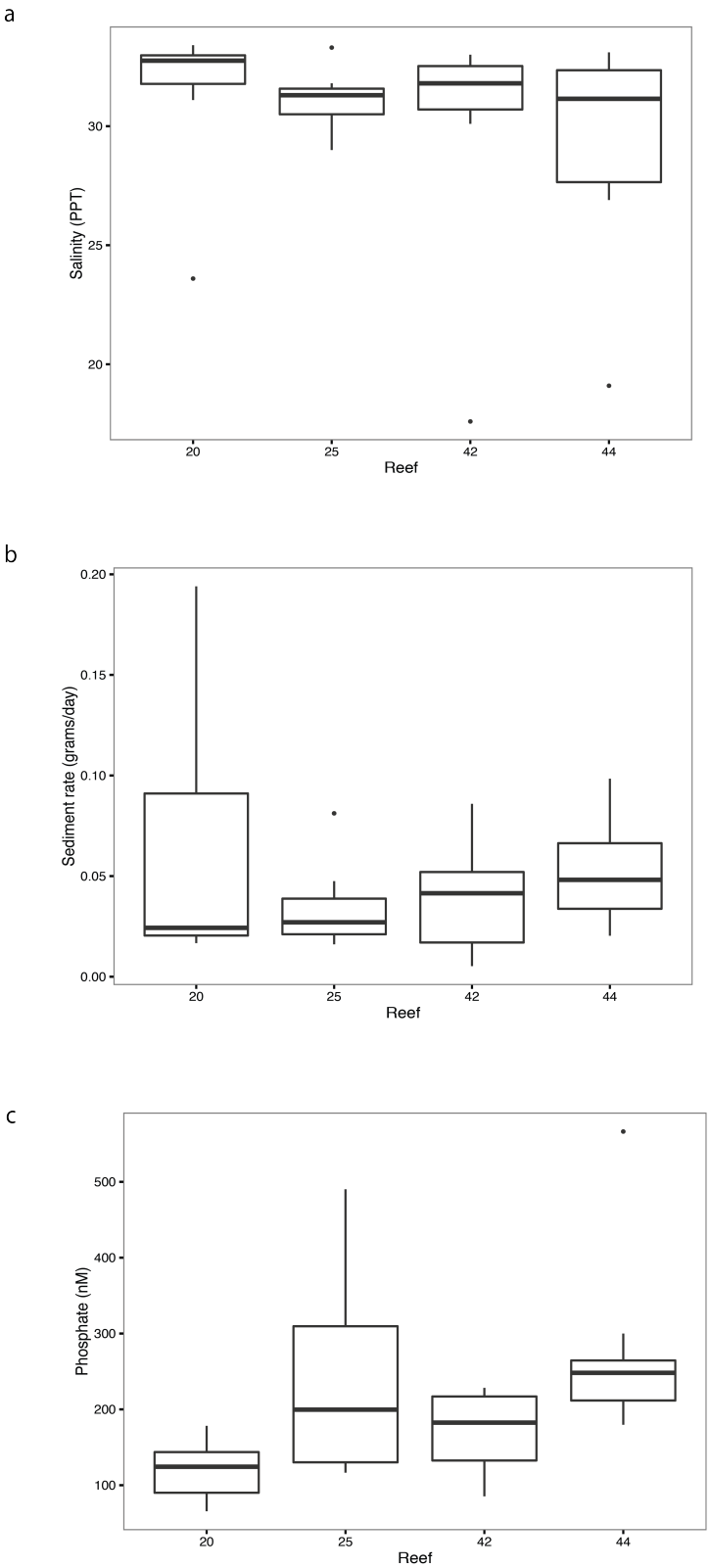

Figure 2.5. Coastal stressor values between patch reefs. a) Salinity, b) Sedimentation rate, c) Phosphate concentration.

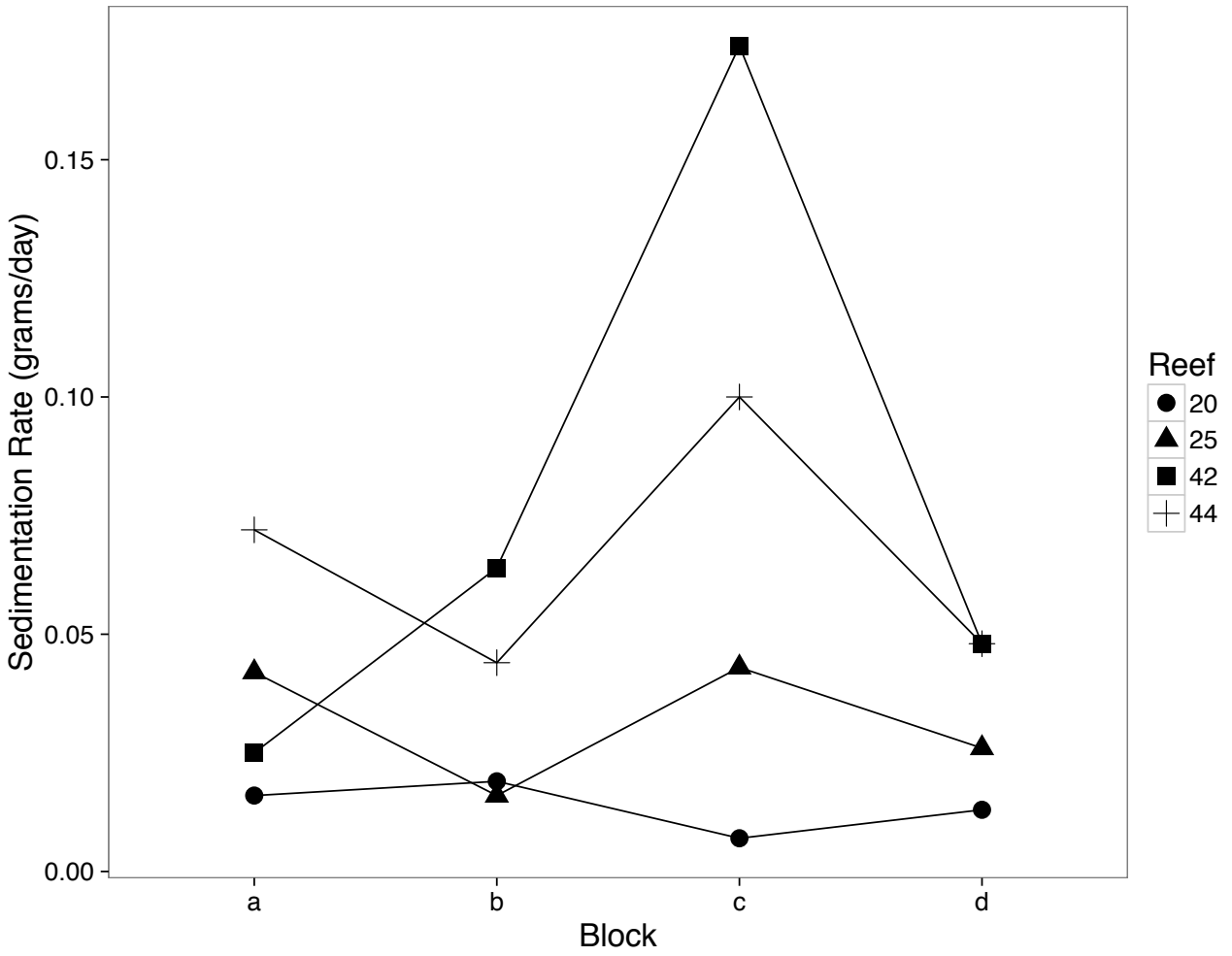

Figure 2.6. Within–reef coastal stressor values. a) Local variation in sedimentation rates by reef (p = 0.0715). b) Local variation in sedimentation rates by block (p = 0.1992).

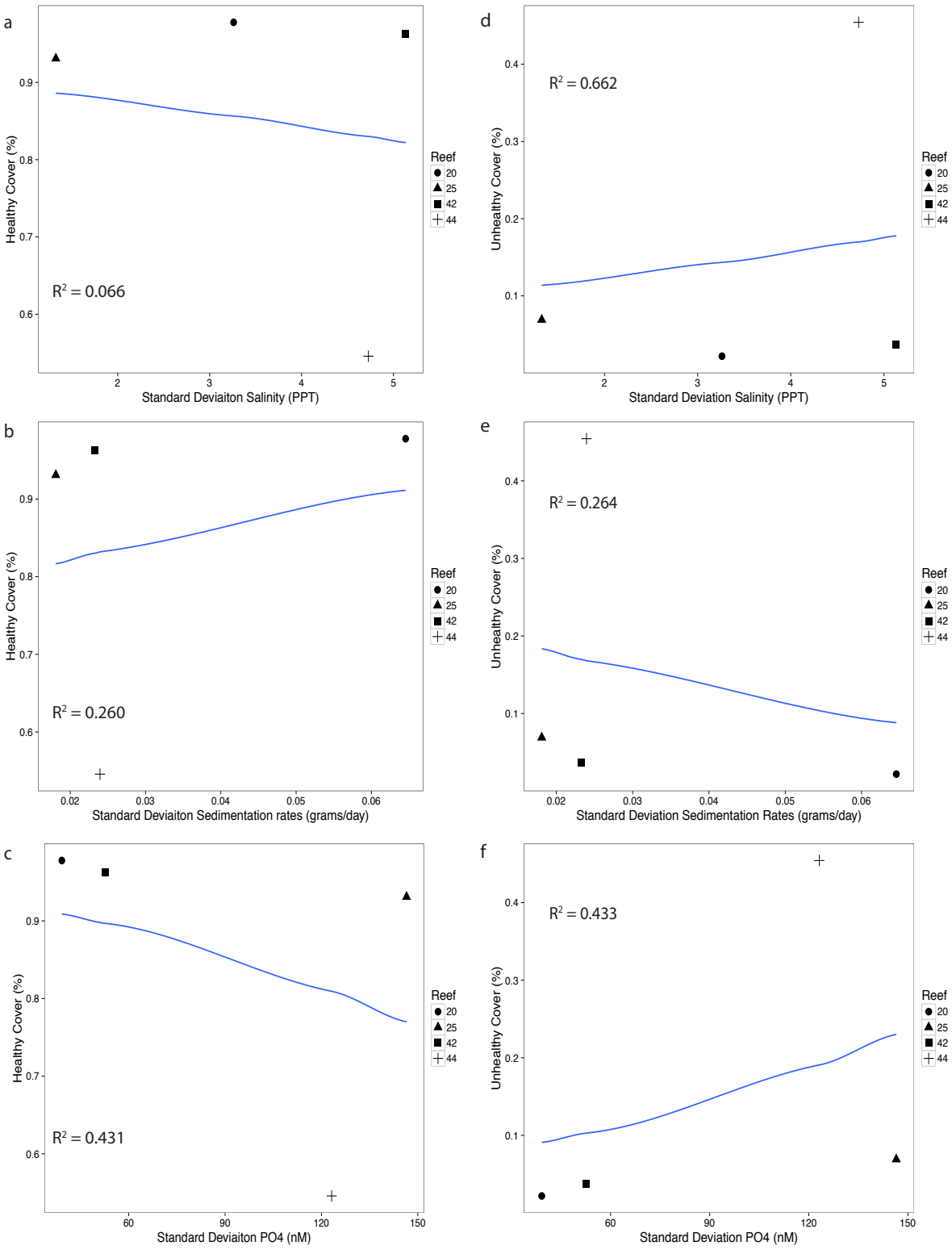

Figure 2.7. Beta model assessing Healthy and Unhealthy coral by the standard deviation of: a, d) salinity, b, e) sedimentation rate, and c, f) phosphate concentration respectively.

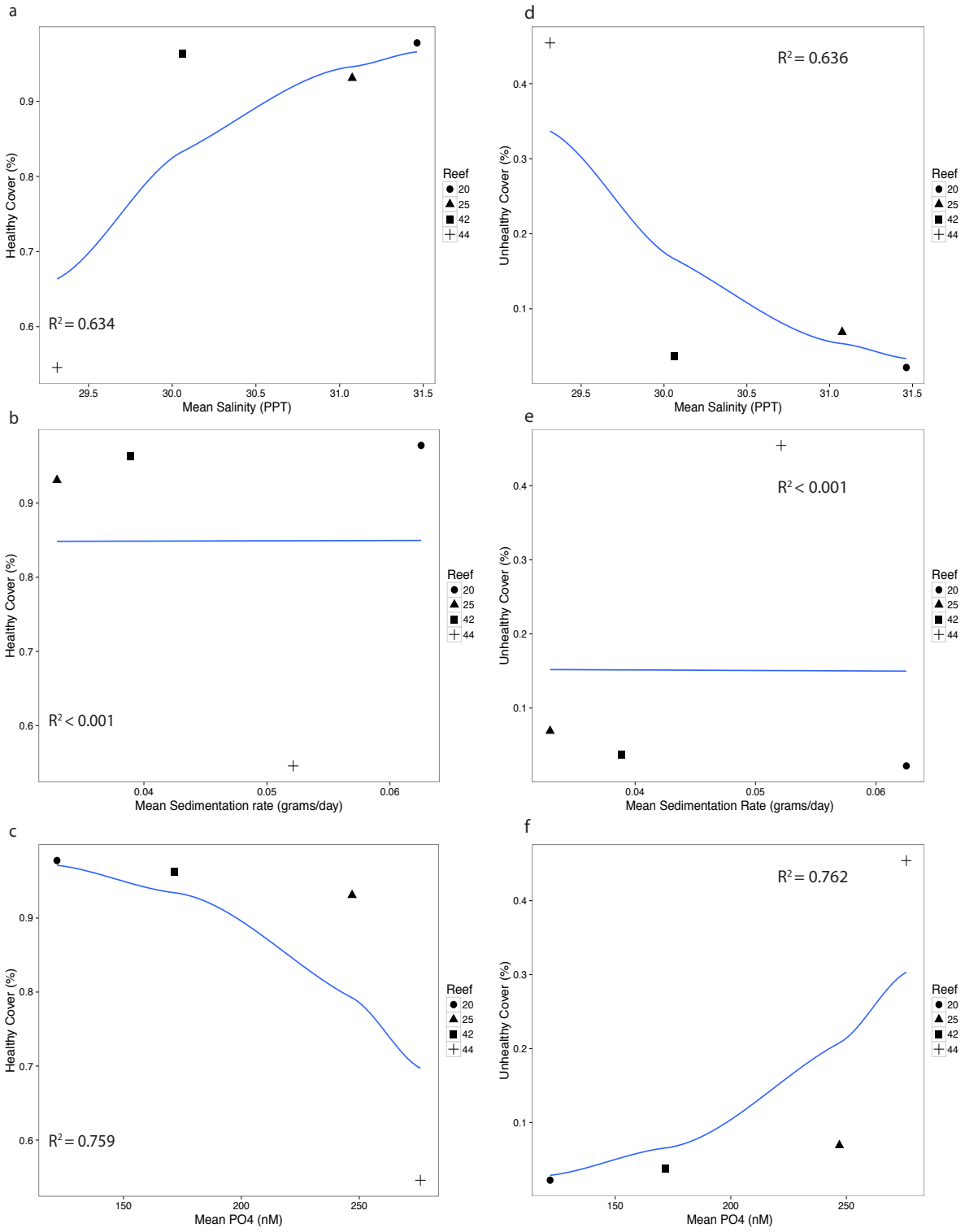

Figure 2.8. Beta model assessing Healthy and Unhealthy coral by mean: a, d) salinity, b, e) sedimentation rate, and c, f) phosphate concentration respectively.

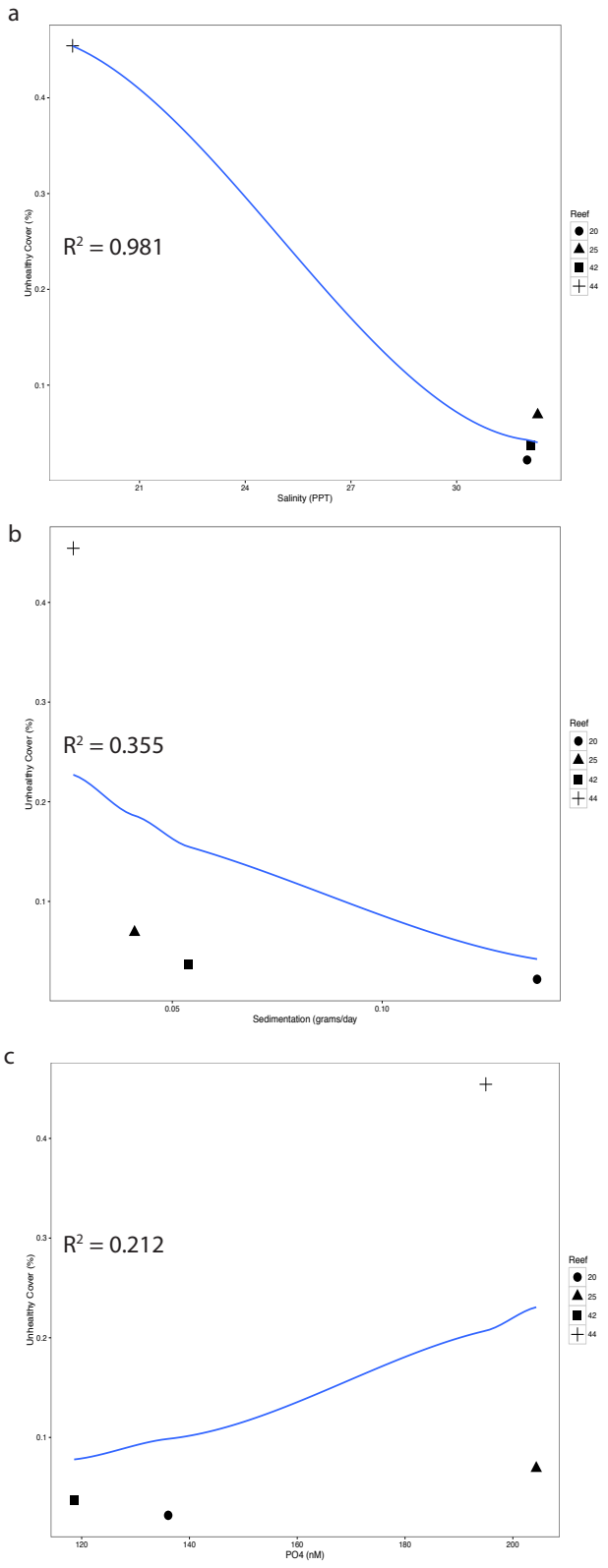

Figure 2.9. Beta model assessing Unhealthy coral at the last time point before reef imagery was collected: a) salinity, b) sedimentation rate, c) phosphate concentration.

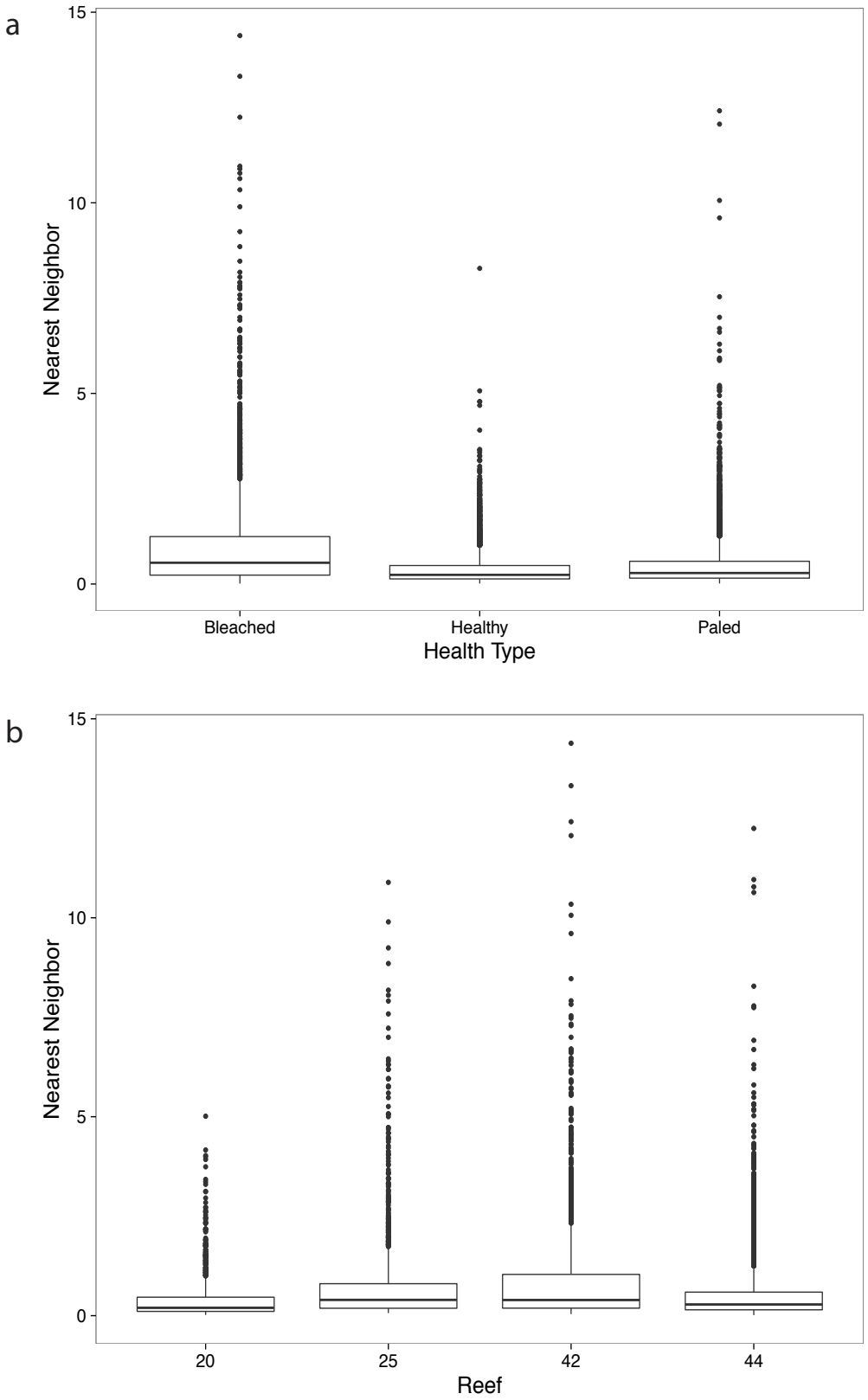

Figure 2.10. Assessing variance of EEN by health type and reef.

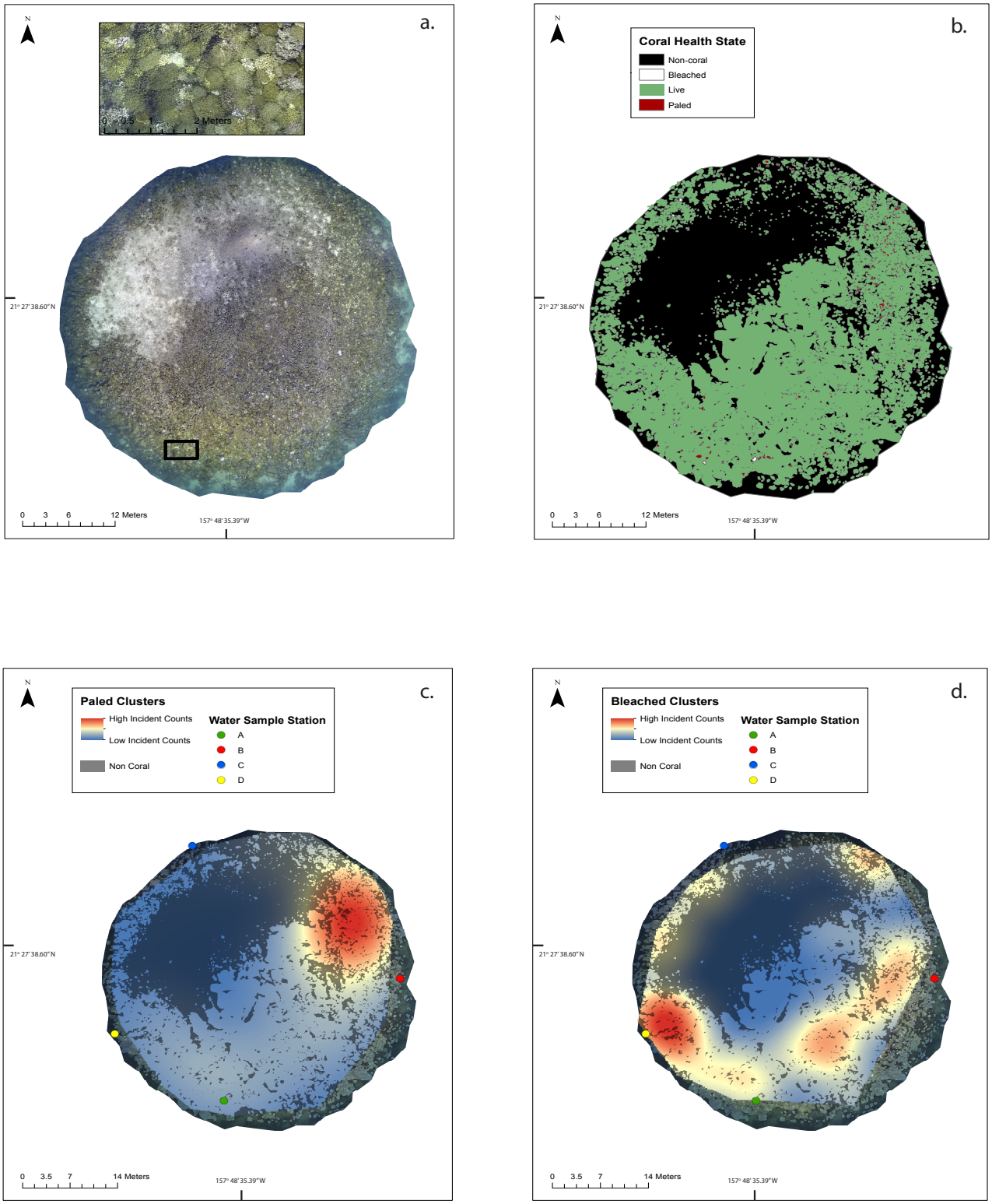

Figure 2.11. Spatial analysis workflow for Reef 20. Pixel size: 0.009 x 0.009 m. a) Reef mosaic with inset. b) Orthomosaic classified into three coral health states and non-coral substrate. c) Heat map of paled colony clusters with environmental sample station locations. d) Heat map of bleached colony clusters with water sample locations

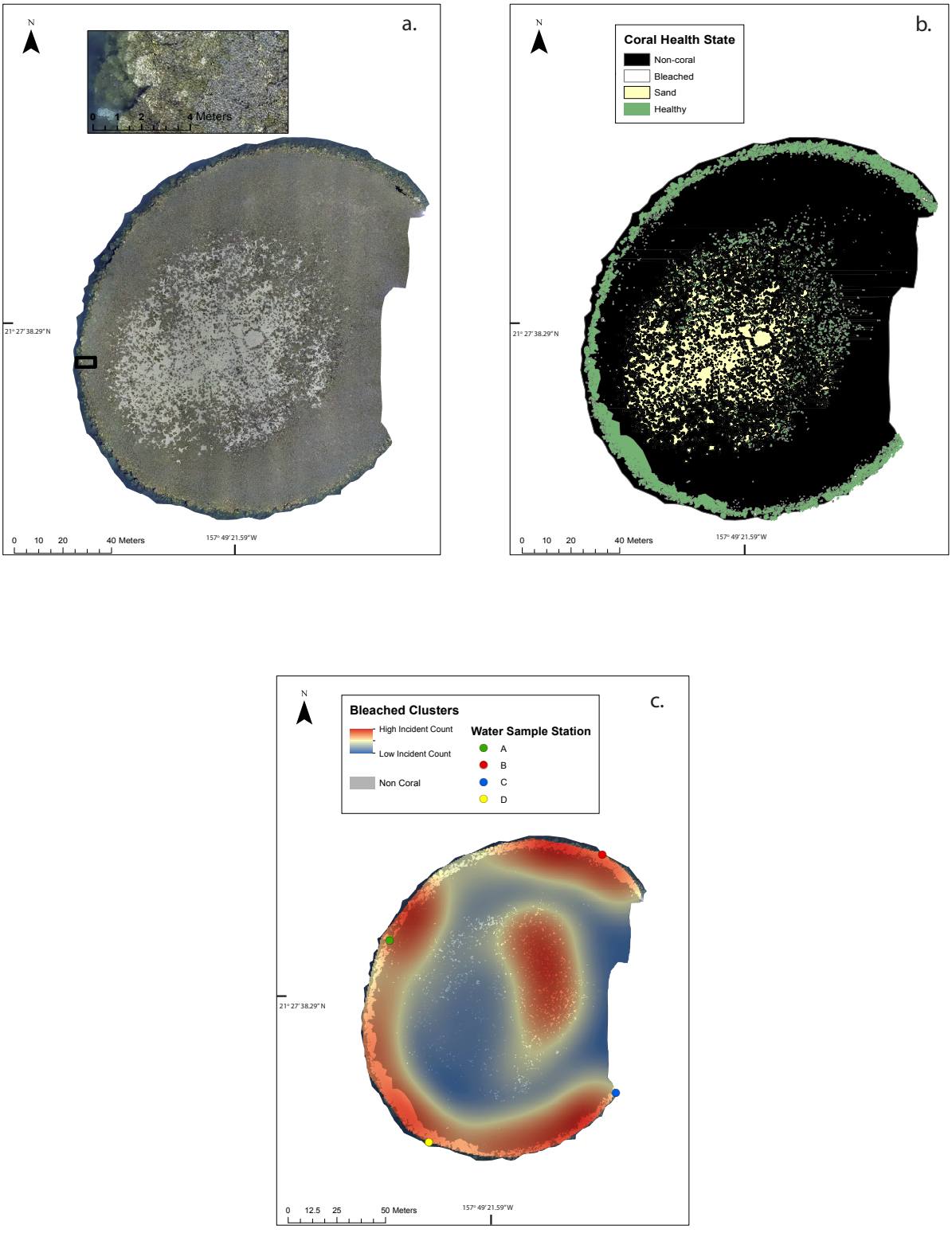

Figure 2.12. Spatial analysis workflow for Reef 25. Pixel size: 0.033 x 0.033 m. a) Reef mosaic with inset. b) Orthomosaic classified into two coral health states, sand, and non-coral substrate. c) Heat map of bleached colony clusters with environmental sample station locations.

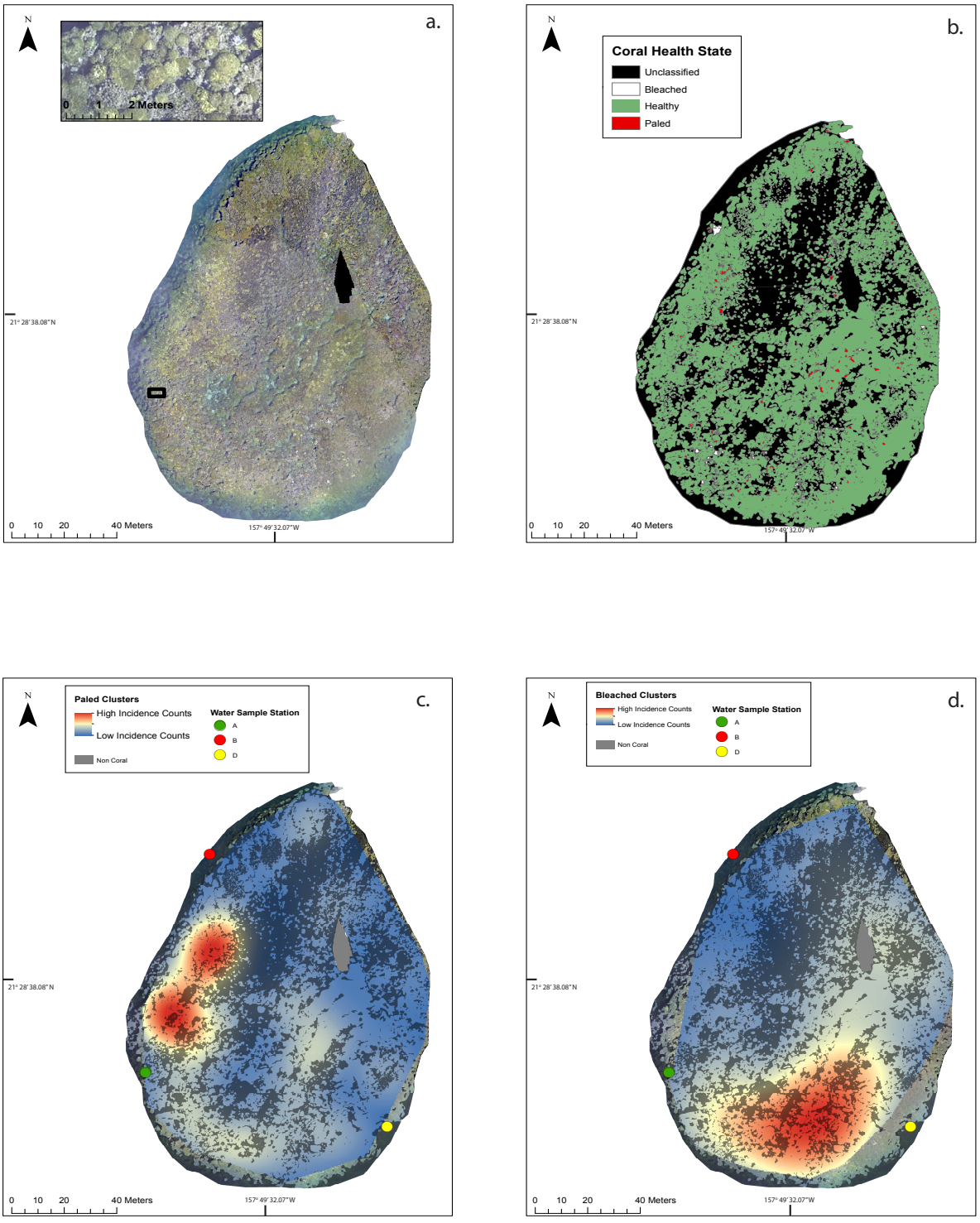

Figure 2.13. Spatial analysis workflow for Reef 42. Pixel size: 0.021 x 0.021 m. a) Reef mosaic with inset. b) Orthomosaic classified into three coral health states and non-coral substrate. c) Heat map of paled colony clusters with environmental sample station locations. d) Heat map of bleached colony clusters with water sample locations. Water sample station C was located beyond extent of reef imagery.

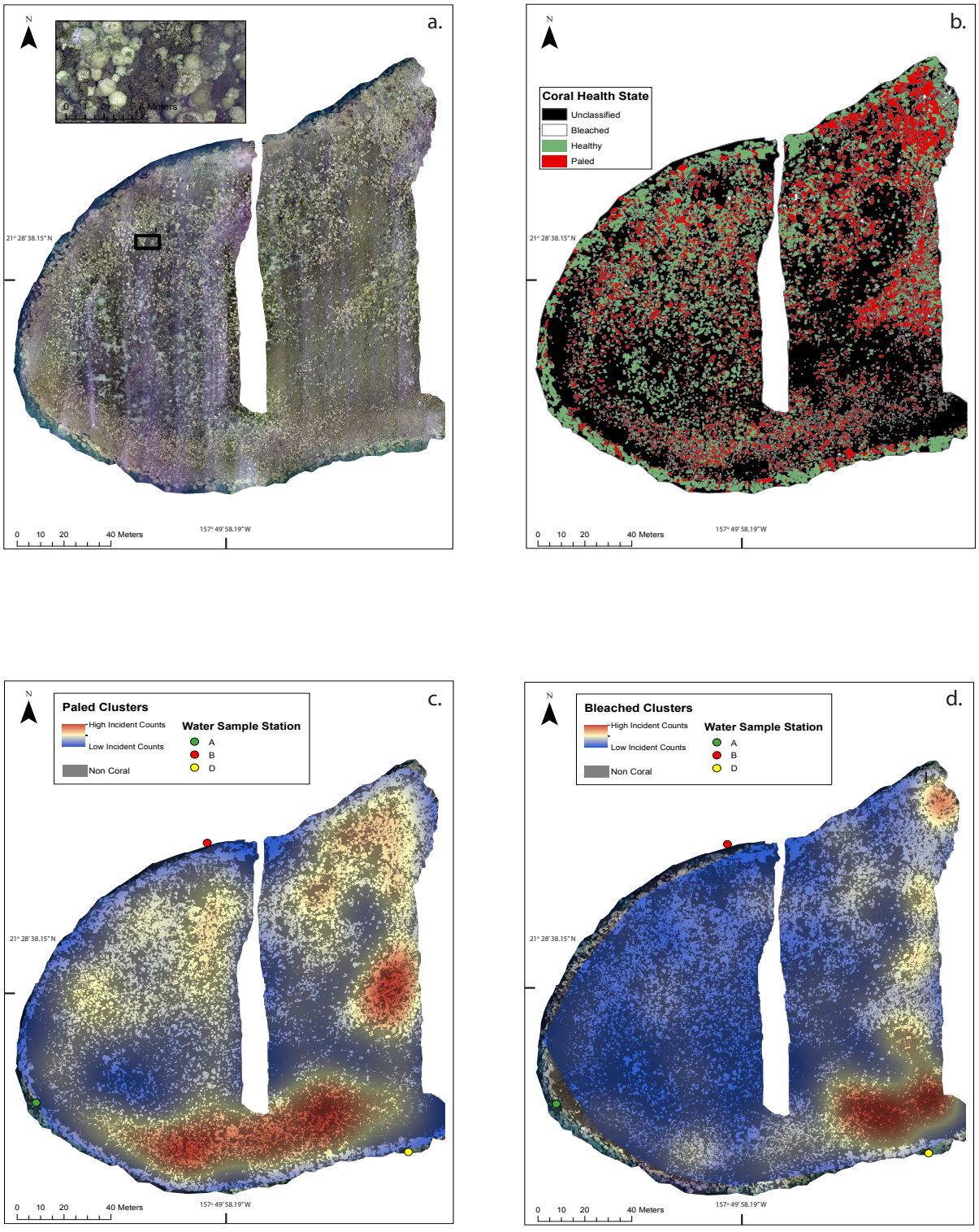

Figure 2.14. Spatial analysis workflow for Reef 44. Pixel size: 0.007 x 0.007 m. a) Reef mosaic with inset. b) Orthomosaic classified into three coral health states and non-coral substrate. c) Heat map of paled colony clusters with environmental sample station locations. d) Heat map of bleached colony clusters with water sample locations. Water sample station C was located beyond extent of reef imagery.

LITERATURE CITED

1. Cesar, H., Burke, L. & Pet-soede, L. The economics of worldwide coral reef degradation. *Atlantic* **14,** 24 (2003).
2. Bozec, Y.-M. & Mumby, P. J. Synergistic impacts of global warming on the resilience of coral reefs. *Proc. R. Soc. B Biol. Sci.* **270,** (2015).
3. Chong-Seng, K. M., Nash, K. L., Bellwood, D. R. & Graham, N. a. J. Macroalgal herbivory on recovering versus degrading coral reefs. *Coral Reefs* **33,** 409–419 (2014).
4. Mora, C. A clear human footprint in the coral reefs of the Caribbean. *Proc. Biol. Sci.* **275,** 767–773 (2008).
5. Hughes, T. P., Graham, N. a J., Jackson, J. B. C., Mumby, P. J. & Steneck, R. S. Rising to the challenge of sustaining coral reef resilience. *Trends Ecol. Evol.* **25,** 633–42 (2010).
6. Riegl, B. M., Sheppard, C. R. C. & Purkis, S. J. Human impact on atolls leads to coral loss and community homogenisation: a modeling study. *PLoS One* **7,** e36921 (2012).
7. Birkeland, C. Geographic comparisons of coral-reef community processes. *Proc. 6th Int. Coral Reef Symp* 211–220 (1988).
8. Doney, S. C. *et al.* Climate Change Impacts on Marine Ecosystems. *Ann. Rev. Mar. Sci.* **4,** 11–37 (2012).
9. Ward, S. & Harrison, P. Changes in gametogenesis and fecundity of acroporid corals that were exposed to elevated nitrogen and phosphorus during the ENCORE experiment. *J. Exp. Mar. Bio. Ecol.* **246,** 179–221 (2000).
10. Hochberg, E. J., Atkinson, M. J. & Andre, S. Spectral reflectance of coral reef bottom-types worldwide and implications for coral reef remote sensing. *Remote Sens. Environ.* **85,** 159–173 (2003).
11. Rowlands, G. *et al.* Satellite imaging coral reef resilience at regional scale. A case-study from Saudi Arabia. *Mar. Pollut. Bull.* **64,** 1222–37 (2012).
12. Jokiel, P. L. *et al.* Comparison of Methods Used to Estimate Coral Cover in the Hawaiian Islands. *Program* 1–22 (2005). doi:10.7717/peerj.954
13. Buddemeier, R. W. & Smith, S. V. Coral adaptation and acclimatization: A most ingenious paradox. *Am. Zool.* **39,** 1–9 (1999).
14. Mumby, P. J., Green, E. P., Edwards, a. J. & Clark, C. D. Coral reef habitat mapping: how much detail can remote sensing provide? *Mar. Biol.* **130,** 193–202 (1997).
15. Turner, W. *et al.* Remote sensing for biodiversity science and conservation. *Trends Ecol. Evol.* **18,** 306–314 (2003).

16. Green, E. P., Mumby, P. J., Edwards, a. J. & Clark, C. D. A review of remote sensing for the assessment and management of tropical coastal resources. *Coast. Manag.* **24,** 1–40 (1996).

17. Hochberg, E. J. & Atkinson, M. J. Capabilities of remote sensors to classify coral, algae, and sand as pure and mixed spectra. *Remote Sens. Environ.* **85,** 174–189 (2003).

18. Goodman, J. & Ustin, S. L. Classification of benthic composition in a coral reef environment using spectral unmixing. *J. Appl. Remote Sens.* **1,** 11501 (2007).

19. Hochberg, E. J. & Atkinson, Æ. M. J. Spectral reflectance of coral. *Cor* **23,** 84–95 (2004).

20. Andréfouët, S. *et al.* Use of in situ and airborne reflectance for scaling-up spectral discrimination of coral reef macroalgae from species to communities. *Mar. Ecol. Prog. Ser.* **283,** 161–177 (2004).

21. Hochberg, E. J., Apprill, A. M., Atkinson, M. J. & Bidigare, R. R. Bio-optical modeling of photosynthetic pigments in corals. *Coral Reefs* **25,** 99–109 (2006).

22. Smith, R. Hyperspectral Imaging. *MicroImages, Inc* 1–24 (2012). doi:10.1016/j.quaint.2007.05.011

23. Kutser, T., Dekker, A. G. & Skirving, W. Modeling spectral discrimination of Great Barrier Reef benthic communities by remote sensing instruments. *Limnol. Oceanogr.* **48,** 497–510 (2003).

24. Myers, M. R., Hardy, J. T., Mazel, C. H. & Dustan, P. Optical spectra and pigmentation of Caribbean reef corals and macroalgae. *Coral Reefs* **18,** 179–186 (1999).

25. Isoun, E., Fletcher, C., Frazer, N. & Gradie, J. Multi-spectral mapping of reef bathymetry and coral cover; Kailua Bay, Hawaii. *Coral Reefs* **22,** 68–82 (2003).

26. Hofmann, G. E. & Gaines, S. D. New Tools to Meet New Challenges: Emerging Technologies for Managing Marine Ecosystems for Resilience. *Bioscience* **58,** 43 (2008).

27. Riitzler, K. Photogrammetry of reef environments by helium balloon. *Coral Reefs Res. methods.* 45–52 (1978).

28. Scoffin, T. P. Reef aerial photography from a kite. *Coral Reefs* **1,** 67–69 (1982).

29. Hardin, P. J. & Jensen, R. R. Small-Scale Unmanned Aerial Vehicles in Environmental Remote Sensing: Challenges and Opportunities. *GIScience Remote Sens.* **48,** 99–111 (2011).

30. Klemas, V. V. Coastal and Environmental Remote Sensing from Unmanned Aerial Vehicles: An Overview. *J. Coast. Res.* **315,** 1260–1267 (2015).

31. Lechner, a. M., Fletcher, a., Johansen, K. & Erskine, P. Characterising Upland Swamps Using Object-Based Classification Methods and Hyper-Spatial Resolution Imagery Derived From an Unmanned Aerial Vehicle. *ISPRS Ann.*

Photogramm. Remote Sens. Spat. Inf. Sci. **I-4,** 101–106 (2012).

32. Cress, B. J. *et al. U . S . Geological Survey Unmanned Aircraft Systems (UAS) Roadmap 2014*. (2015).

33. Pierce, G., Iv, J., Pearlstine, L. G. & Percival, H. F. An Assessment of Small Unmanned Aerial Vehicles for Wildlife Research. *BioOne* **34,** 750–758 (2006).

34. Martin, J. *et al.* Estimating Distribution of Hidden Objects with Drones: From Tennis Balls to Manatees. *PLoS One* **7,** e38882 (2012).

35. Hodgson, A., Kelly, N. & Peel, D. Unmanned aerial vehicles (UAVs) for surveying Marine Fauna: A dugong case study. *PLoS One* **8,** 1–15 (2013).

36. Chirayath, V. & Earle, S. Drones that See Through Waves - Developing New Tools in Coastal Marine Conservation. *Aquat. Conserv. Mar. Freshw. Ecosyst.* **Special Is,** (2016).

37. Hodgson, J. C., Baylis, S. M., Mott, R., Herrod, A. & Clarke, R. H. Precision wildlife monitoring using unmanned aerial vehicles. *Sci. Rep.* **6,** 22574 (2016).

38. Jokiel, P. L. Illustrated Scientific Guide To Kane'ohe Bay, O'ahu. 65

39. Neilson, B., Blodgett, J., Gewecke, C., Stubbs, B. & Tejchma, K. *Kaneohe Bay , Oahu Snap-Assessment Report*. (2014).

40. Westoby, M. J., Brasington, J., Glasser, N. F., Hambrey, M. J. & Reynolds, J. M. 'Structure-from-Motion' photogrammetry: A low-cost, effective tool for geoscience applications. *Geomorphology* **179,** 300–314 (2012).

41. Burns, J., Delparte, D., Gates, R. & Takabayashi, M. Integrating structure-from-motion photogrammetry with geospatial software as a novel technique for quantifying 3D ecological characteristics of coral reefs. *PeerJ* **3,** e1077 (2015).

42. Stal, C., Bourgeois, J., Maeyer, P. De, Mulder, G. De & Wulf, A. De. Test Case on the Quality Analysis of Structure from Motion in Airborne Applications. (2012).

43. Duce, S. *et al.* A morphometric assessment and classification of coral reef spur and groove morphology. *Geomorphology* **265,** 68–83 (2016).

44. Wilkinson, C. Status of Coral Reefs of the World: 2008. *Status Coral Reefs World 2008* 1–297 (2008).

45. Smith, C. & Alberte, R. . Characterization of in Vigo absorption features of cholorphyte, phaeophyte and rhodophyte algal species. **552,** 543–552 (1993).

46. Aguirre-Gomez, R., Boxall, S. R. & Weeks, a. R. Detecting photosynthetic algal pigments in natural populations using a high-spectral-resolution spectroradiometer. 37–41 (2001). doi:10.1080/014311601316958380

47. Jeffrey, S. W. & Haxo, F. T. Photosyntheic Pigments of Symbiotic Dinoflagelates from Corals and Clams. (1966).

48. Govan, R. *Educational Use of Unmanned Aircraft Systems (UAS)*. **May 4th,** (2016).

49. Federal Aviation Administration. Summary of Small Unmanned Aircraft Rule (Part 107). (2016).

50. FAA. *Operation and Certification of Small Unmanned Aircraft Systems*. *Department of Transportation* 1–624 (2015). doi:10.1017/CBO9781107415324.004

51. Chapin, F. S. *et al.* Consequences of changing biodiversity. *Nature* **405,** 234–242 (2000).

52. Muthukrishnan, R. & Fong, P. Multiple anthropogenic stressors exert complex , interactive effects on a coral reef community. *Coral Reefs* 911–921 (2014). doi:10.1007/s00338-014-1199-1

53. Bellwood, D. R., Hughes, T. P., Folke, C. & Nyström, M. Confronting the coral reef crisis. *Nature* **429,** 827–833 (2004).

54. Jokiel, P. L., Hunter, C. L., Taguchi, S. & Watarai, L. Ecological impact of a fresh-water 'reef kill' in Kaneohe Bay, Oahu, Hawaii. *Coral Reefs* **12,** 177–184 (1993).

55. Risk, M. J. Assessing the effects of sediments and nutrients on coral reefs. *Curr. Opin. Environ. Sustain.* **7,** 108–117 (2014).

56. Ward, J. V. Riverine landscapes: Biodiversity patterns, disturbance regimes, and aquatic conservation. *Biol. Conserv.* **83,** 269–278 (1998).

57. Rodgers, K. S., Kido, M. H., Jokiel, P. L., Edmonds, T. & Brown, E. K. Use of integrated landscape indicators to evaluate the health of linked watersheds and coral reef environments in the Hawaiian Islands. *Environ. Manage.* **50,** 21–30 (2012).

58. Banner, A. H. Kaneohe Bay: urban pollution and a coral reef system. in *Proceedings of the Second International Coral Reef Symposium. Vol. 2.* 685–702 (1974).

59. Downs, C. a., Woodley, C. M., Richmond, R. H., Lanning, L. L. & Owen, R. Shifting the paradigm of coral-reef 'health' assessment. *Mar. Pollut. Bull.* **51,** 486–494 (2005).

60. Obura, D. & Grimsditch, G. *Resilience Assessment of Coral Reefs bleaching and thermal stress*. *Resilience Assessment of Coral Reefs* (2009).

61. Graham, N. A. J., Jennings, S., Macneil, M. A., Mouillot, D. & Wilson, S. K. Predicting climate-driven regime shifts versus rebound potential in coral reefs. *Nature* (2015). doi:10.1038/nature14140

62. Baker, A. C., Glynn, P. W. & Riegl, B. Climate change and coral reef bleaching: An ecological assessment of long-term impacts, recovery trends and future outlook. *Estuar. Coast. Shelf Sci.* **80,** 435–471 (2008).

63. Lesser, M. P. Oxidative stress in marine environments: biochemistry and physiological ecology. *Annu. Rev. Physiol.* **68,** 253–278 (2006).

64. Glynn, P. El Nino-associated disturbance to coral reefs and post disturbance mortality by Acanthaster planci . *Mar. Ecol. Prog. Ser.* **26,** 295–300 (1985).

65. Harriott, V. Mortality rates of scleractinian corals before and during a mass bleaching event. *Mar. Ecol. Prog. Ser.* **21,** 81–88 (1985).

66. Brown, B. E. Coral bleaching: causes and consequences. *Coral Reefs* **16,** 129–138 (1997).

67. Bahr, K. D., Jokiel, P. L. & Rodgers, K. S. The 2014 coral bleaching and freshwater flood events in Kāne'ohe Bay, Hawai'i. *PeerJ* **3,** e1136 (2015).

68. Bahr, K. D., Jokiel, P. L. & Toonen, R. J. The unnatural history of Kāne'ohe Bay: coral reef resilience in the face of centuries of anthropogenic impacts. *PeerJ* **3,** e950 (2015).

69. Lowe, R. J., Falter, J. L., Monismith, S. G. & Atkinson, M. J. A numerical study of circulation in a coastal reef-lagoon system. *J. Geophys. Res. Ocean.* **114,** 1–18 (2009).

70. Kuffner, I. B. Temporal variation in photosynthetic pigments and UV-absorbing compounds in shallow populations of two hawaiian reef corals. *Pacific Sci.* **59,** 561–580 (2005).

71. Wolanski, E., Martinez, J. a. & Richmond, R. H. Quantifying the impact of watershed urbanization on a coral reef: Maunalua Bay, Hawaii. *Estuar. Coast. Shelf Sci.* **84,** 259–268 (2009).

72. Laws, E. A. & Ferentinos, L. Human impacts on fluxes of nutrients and sediment in waimanalo stream, O'ahu, Hawaiian Islands. *Pacific Sci.* **57,** 119–140 (2003).

73. Hunter, C. L. & Evans, C. Coral Reefs in Kaneohe Bay, Hawaii: Two centuries of western influence and two decades of data. *Bull. Mar. Sci.* **57,** 501–515 (1995).

74. Johns, K. a., Osborne, K. O. & Logan, M. Contrasting rates of coral recovery and reassembly in coral communities on the Great Barrier Reef. *Coral Reefs* **33,** 553–563 (2014).

75. US Climate Data. (2015). Available at: http://www.usclimatedata.com/climate/kaneohe-bay/hawaii/united-states/ushi0064.

76. McCook, L., Jompa, J. & Diaz-Pulido, G. Competition between corals and algae on coral reefs: a review of evidence and mechanisms. *Coral Reefs* **19,** 400–417 (2014).

77. Padilla-Gamiño, J. L. *et al.* Sedimentation and the reproductive biology of the hawaiian reef-building coral Montipora capitata. *Biol. Bull.* **226,** 8–18 (2014).

78. Peters, E. C. & Pilson, M. E. Q. A comparative study of the effects of sedimentation on symbiotic and asymbiotic colonies of the coral Astrangiadanae Milne Edwards and Haime 1849. *J. Exp. Mar. Bio. Ecol.* **92,** 215–230 (1985).

79. Riegl, B. Effects of sediment on the energy budgets of four scleractinian (Bourne

1900) and five alcyonacean (L amouroux 18 16) corals. *J. Exp. Mar. Bio. Ecol.* **186,** 259–275 (1995).

80. Satoru, T. Sedimentation of newly produced particulate organic matter in a subtropical inlet, Kaneohe Bay, Hawaii. *Estuar. Coast. Shelf Sci.* **14,** 533–544 (1982).

81. Mumby, P. J., Chisholm, J. R. M., Edwards, A. J., Andrefouet, S. & Jaubert, J. Cloudy weather may have saved Society Island reef corals during the 1998 ENSO event. *Mar. Ecol. Prog. Ser.* **222,** 209–216 (2001).

82. Golbuu, Y. *et al.* Palau's coral reefs show differential habitat recovery following the 1998-bleaching event. *Coral Reefs* **26,** 319–332 (2007).

83. Smith, J. E., Smith, C. M. & Hunter, C. L. An experimental analysis of the effects of herbivory and nutrient enrichment on benthic community dynamics on a Hawaiian reef. *Coral Reefs* **19,** 332–342 (2001).

84. Bruno, J. F., Petes, L. E., Harvell, C. D. & Hettinger, A. Nutrient enrichment can increase the severity of coral diseases. *Ecol. Lett.* **6,** 1056–1061 (2003).

85. Vega Thurber, R. L. *et al.* Chronic nutrient enrichment increases prevalence and severity of coral disease and bleaching. *Glob. Chang. Biol.* **20,** 544–554 (2014).

86. Cox, E. F. & Ward, S. Impact of elevated ammonium on reproduction in two Hawaiian scleractinian corals with different life history patterns. *Mar. Pollut. Bull.* **44,** 1230–5 (2002).

87. Stambler, N. & Stimson, J. Effects of Nutrient Enrichment and Water Motion on the Coral Pocillopora damicornis '. *Pacific Sci.* **45,** 299–307 (1991).

88. Smith, S. V, Kimmerer, W. J., Laws, E. a, Brock, R. E. & Walsh, T. W. Kaneohe Bay sewage diversion experiment: perspectives on ecosystem responses to nutritional perturbation. *Pacific Sci.* **35,** 279–395 (1981).

89. Lowe, R. J., Falter, J. L., Monismith, S. G. & Atkinson, M. J. A numerical study of circulation in a coastal reef-lagoon system. *J. Geophys. Res. Ocean.* **114,** (2009).

90. Atkinson, M. J. & Bilger, R. W. Effects of water velocity on phosphate uptake in coral reef-flat communities. *Limnol. Ocean.* **37,** 273–279 (1992).

91. Patterson, M. R., Sebens, K. P. & Olson, R. R. In situ measurements of flow effects on primary production and dark respiration in reef corals. *Limnol. Oceanogr.* **36,** 936–948 (1991).

92. Conklin, E. J. & Smith, J. E. Abundance and spread of the invasive red algae, Kappaphycus spp., in Kane'ohe Bay, Hawai'i and an experimental assessment of management options. *Biol. Invasions* **7,** 1029–1039 (2005).

93. Work, T. *Diagnostic Case Report*. (2015).

94. Strickland, J. D. H. & Parsons, T. R. A Practical Handbook of Seawater Analysis. *A Pract. Handb. seawater Anal.* **167,** 185 (1972).

95. Storlazzi, C. D., Dartnell, P., Hatcher, G. A. & Gibbs, A. E. End of the chain? Rugosity and fine-scale bathymetry from existing underwater digital imagery using structure-from-motion (SfM) technology. *Coral Reefs* **35,** 887–892 (2016).

96. Kuznetsova, A., Brockhoff, P. B. & Christensen, R. H. B. *Tests in Linear Mixed Effects Models Version*. (2016). doi:https://CRAN.R-project.org/package=lmerTest

97. Cribari-Neto, F. & Zeileis, A. Beta regression in R. *J. Stat. Softw.* **34,** 24 (2010).

98. Mcgarigal, K. *Fragstats.Help.4.2*. (2015). doi:10.1016/S0022-3913(12)00047-9

99. Ritson-Williams & Gates. Kaneohe Bay Seawater Temperature Data 2014 and 2015 - superseded. doi:10.5281/zenodo.46366

100. Coles, S. L. & Jokiel, P. L. Synergistic Effects of Temperature , Salinity and Light on the Hermatypic Coral Montipora verrucosa. *Mar. Biol.* **49,** 187–195 (1978).

101. Humanes, A. *et al.* Cumulative Effects of Nutrient Enrichment and Elevated Temperature Compromise the Early Life History Stages of the Coral Acropora tenuis. *PLoS One* **11,** 215–27 (2016).

102. Smith, J. E., Hunter, C. L. & Smith, C. M. The effects of top–down versus bottom–up control on benthic coral reef community structure. *Oecologia* **163,** 497–507 (2010).

103. Larned, S. T. Nitrogen- versus phosphorus-limited growth and sources of nutrients for coral reef macroalgae. *Mar. Biol.* **132,** 409–421 (1998).